Sub-Basin-Scale Variability in the Interior of the Ocean: Waves, Eddies, and Turbulence

- The locally measurable reality.

  "Climate is what you expect; weather is what you get."

  (Mark Twain)

- Manifestations of many distinctive processes.

  Interesting scientific topics, generally more accessible to measurements, modeling, and theory than the global circulation.

- Primary modes of material transport and momentum flux at space and time scales below the mean and seasonal basin circulations.

  Necessary components of OGCMs, mostly as parameterizations.

Categories: synoptic ($L \sim 1000$ km, $T \sim 1$ day)

mesoscale ($L \sim 30 - 200$ km, $H \ll L$, $Ro \ll 1$)

submesoscale ($L \sim 0.1 - 10$ km, $H \ll L$, $Ro \sim 1$)

microscale ($L < 30$ m, $H \sim L$, $Ro \gg 1$)

.

Concept: The ocean, like the atmosphere and nearly all natural fluids, is full of variability.

Because its volume is so large and its molecular diffusion and dissipation scales are so small, its wavenumber spectrum is quite broad, spanning ≈ 10 decades.

From surface capillary waves ($t \sim 10^{-2}$ s) to the global thermohaline adjustment time ($t \sim 3 \times 10^{11}$ s) its intrinsic-variability frequency spectrum is also quite broad, spanning ≈ 13 decades. On even longer time scales, the climate and ocean are forced by astronomy and geology.

Most oceanic variability is intrinsic, not forced; $i.e.,$ it arises from fluid instabilities of more directly forced flows.

It seems generally characteristic of natural fluids that the spectra are red; $i.e.,$ larger variance is associated larger scales and lower frequencies.

Across the scale range, many different physical influences — stratification, rotation, boundary shape, shear — appear in different combinations, hence the range of phenomena is quite varied.

The Zoo: Interior Variability Phenomena

- sound waves ($c_s \approx 1500$ m s^{-1})
- shallow-water (long) gravity waves ($c_g = \sqrt{gh}$)
- inertia-gravity waves and internal tide (frequencies $f \leq \sigma \leq N$)
- (Quasigeostrophic) Rossby and topographic waves ($\sigma \propto \nabla_h Q \neq 0$; $Q = (f_o + \beta y)/h(x,y)$)
- equatorial ($f_o = 0$, $\beta \neq 0$) and coastal ($f_o \neq 0$, $\beta = 0$) Kelvin waves
- baroclinic and barotropic instabilities of "mean" currents (Rayleigh criterion: $\nabla_h \overline{Q}$ changes sign; $\overline{Q} = f(y) + \hat{\mathbf{z}} \cdot \nabla \times \overline{\mathbf{u}}_h + \partial_z (f\overline{b}/N^2)$)
- tropical instability waves (TIW)
- mesoscale eddies and geostrophic turbulence (N, f, and β with $Ro, Fr \ll 1$)
- submesoscale fronts and filaments ($Ro, Fr \sim 1$)
- phytoplankton patchiness controlled by submesoscale flow

- island and topographic wakes, flow separation, and instabilities
- submesoscale coherent vortices (SCVs)
- centrifugal instability (Q changes sign; $Q = (f\hat{\mathbf{z}} + \nabla \times \mathbf{u}) \cdot (\hat{\mathbf{z}} \int N^2\, dz + \nabla b)$)
- stratified turbulence (N without f)
- stratified shear instability (Kelvin-Helmholtz; $Ri = N^2/(\partial_z \mathbf{u})^2 < 1$)
- double diffusion (molecular diffusivity $\kappa_T \approx 100\, \kappa_S$ in seawater)
- micro-structure turbulence, mixing, and dissipation (cascade to very small scales uninfluenced by N and f but ultimately influenced by molecular ν and κ)

The Flow of Energy Through the Ocean
(non-tidal and non-surface wave)

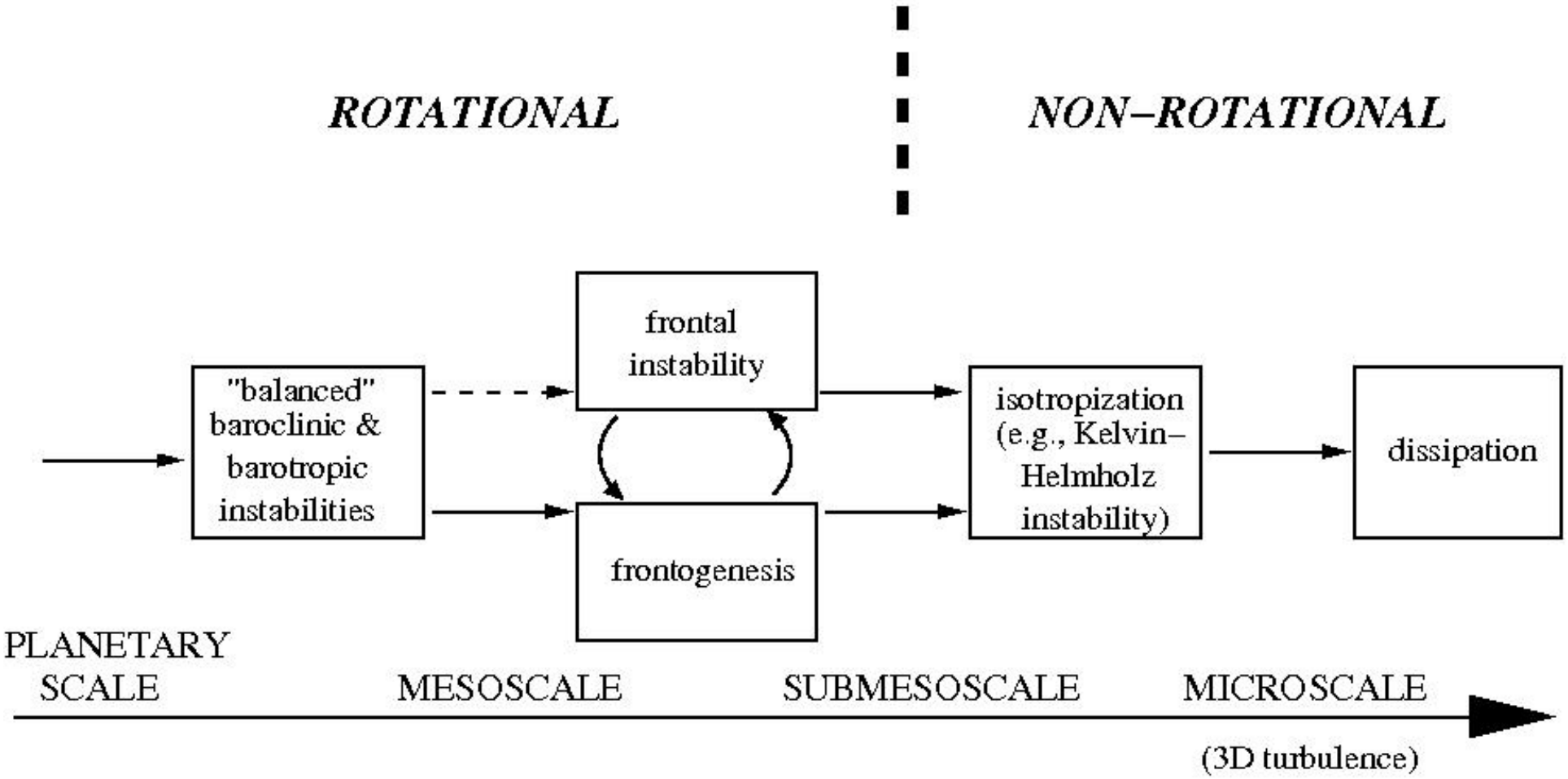

Isopycnal and Diapycnal Transport

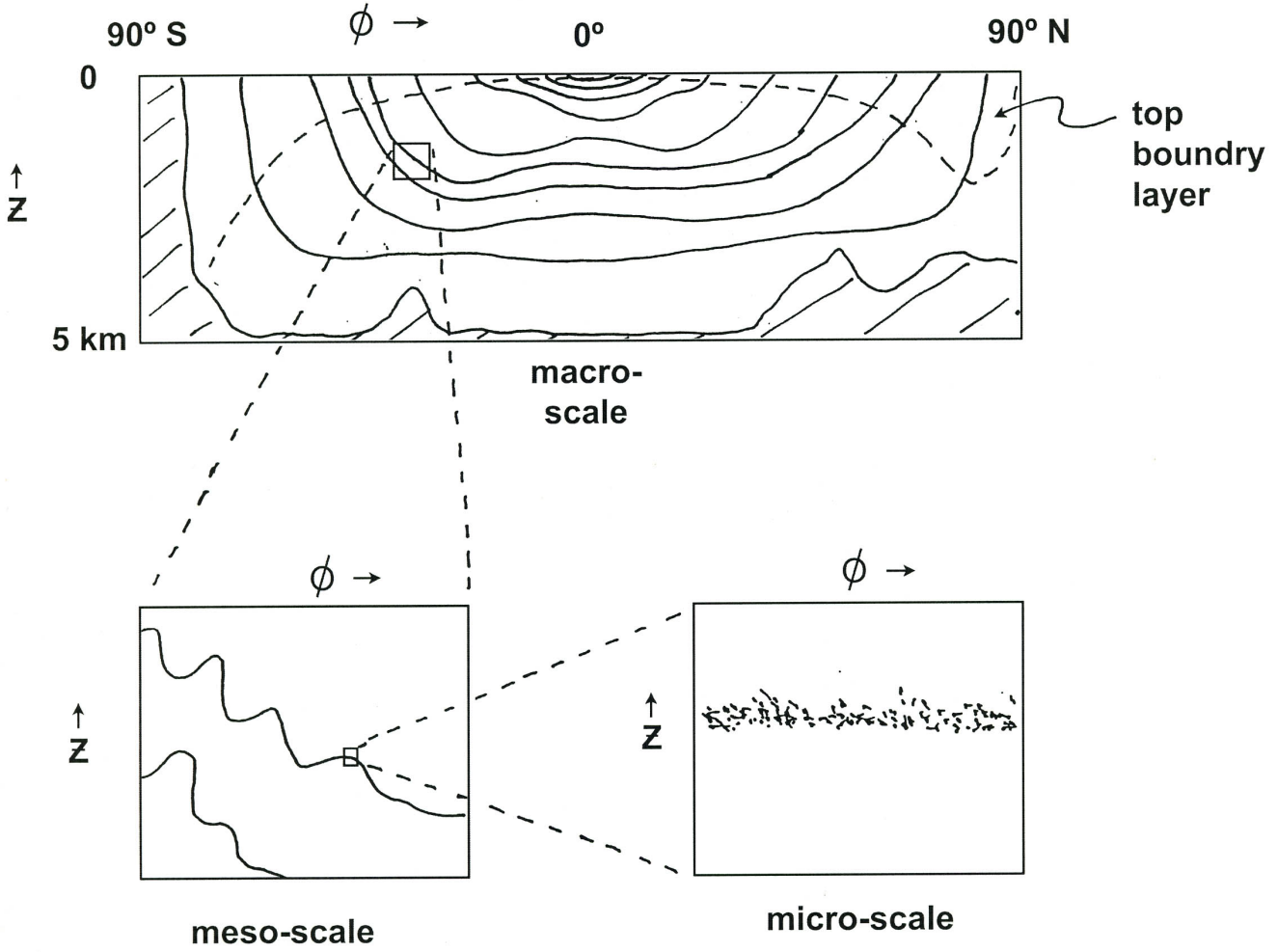

Schematic meridional section of potential density surfaces viewed on three different spatial scales. The largest scale shows the time-mean or low-frequency structure. The intermediate scale shows how eddies and inertia-gravity deform the large-scale buoyancy structure on time scales of hours to months. The finest scale shows how small-scale turbulence mixes the parcels and disrupts the strict vertical ordering of $b(z)$ on a time scale of minutes. (This is a repeated figure.)

Eddy diffusivity estimates of transport efficiency: $\kappa_{iso} \sim 10^3$ m^2 s^{-1}; $\kappa_{v,bl} \sim 10^{-3} - 10^{-2}$ m^2 s^{-1}; $\kappa_{dia} \sim 10^{-5}$ m^2 s^{-1}. (Remember ∇^2 factors of L^{-2} horizontally $\ll H^{-2}$ vertically.)

Storm Surge

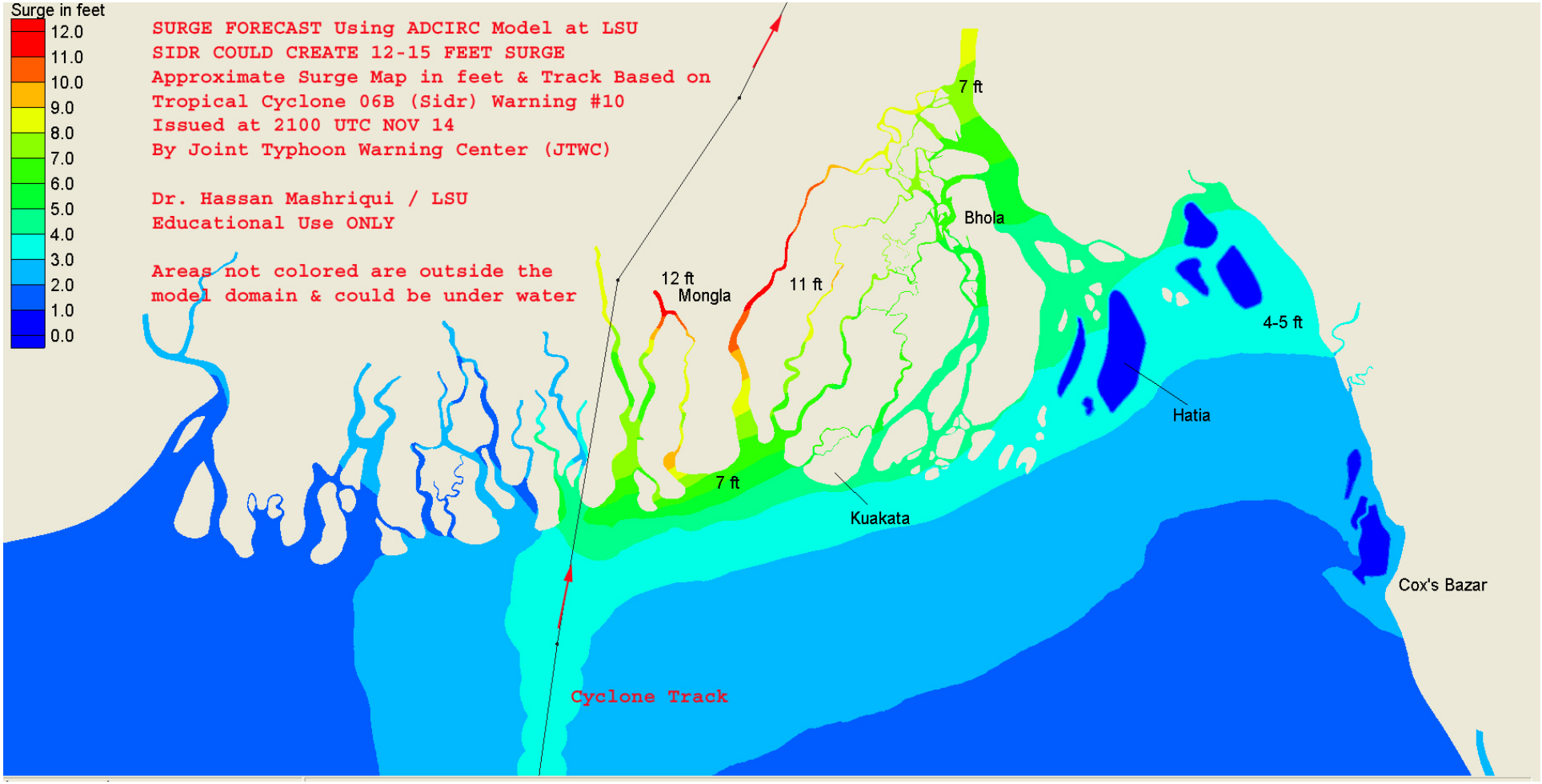

Prediction of sea level anomaly [ft] near Bangladesh in November 2008. The basis is a shallow-water model with wind stress and tides. Surges happen when there is phase coincidence of the two forcings and free-surface gravity wave propagation ($c_g = \sqrt{gh}$) that focuses the "slosh" onto a shoreline sector. This case is for a tropical cyclone (typhoon) coming onto land. Tsunamis have a similar dynamics caused by earthquakes.

Inertia-Gravity Waves

- Waves due to rotation f and stable stratification $N(z)$; period ≈ 1 hour - 1 day.

- Approximately a linear dynamics for fluctuations about a stratified resting state, *e.g.*,

$$\frac{\partial \mathbf{u}'}{\partial t} + f\hat{\mathbf{z}} \times \mathbf{u}' \;=\; -\nabla\phi' + b'\hat{\mathbf{z}}\,, \quad \frac{\partial b'}{\partial t} + w'N^2 \;=\; 0\,, \quad \nabla \cdot \mathbf{u}' \;=\; 0\,.$$

- Wave eigenmodes $\propto e^{i\sigma t}$ have frequencies between f and N.

- Generated by wind-changes, radiation from BL turbulence, and stratified flow over topography (especially tides).

- Nearly universal "saturated" spectrum in $(\sigma, \mathbf{k})$ due to weak nonlinear interaction among wave modes (a.k.a. the Garrett-Munk spectrum). But there are "hot spots", especially in relation to tidal flows through straits and over ridges.

- An important cause of diapycnal mixing due to turbulence arising from wave breaking in the interior $\rightarrow$ overtuning of stable stratification.

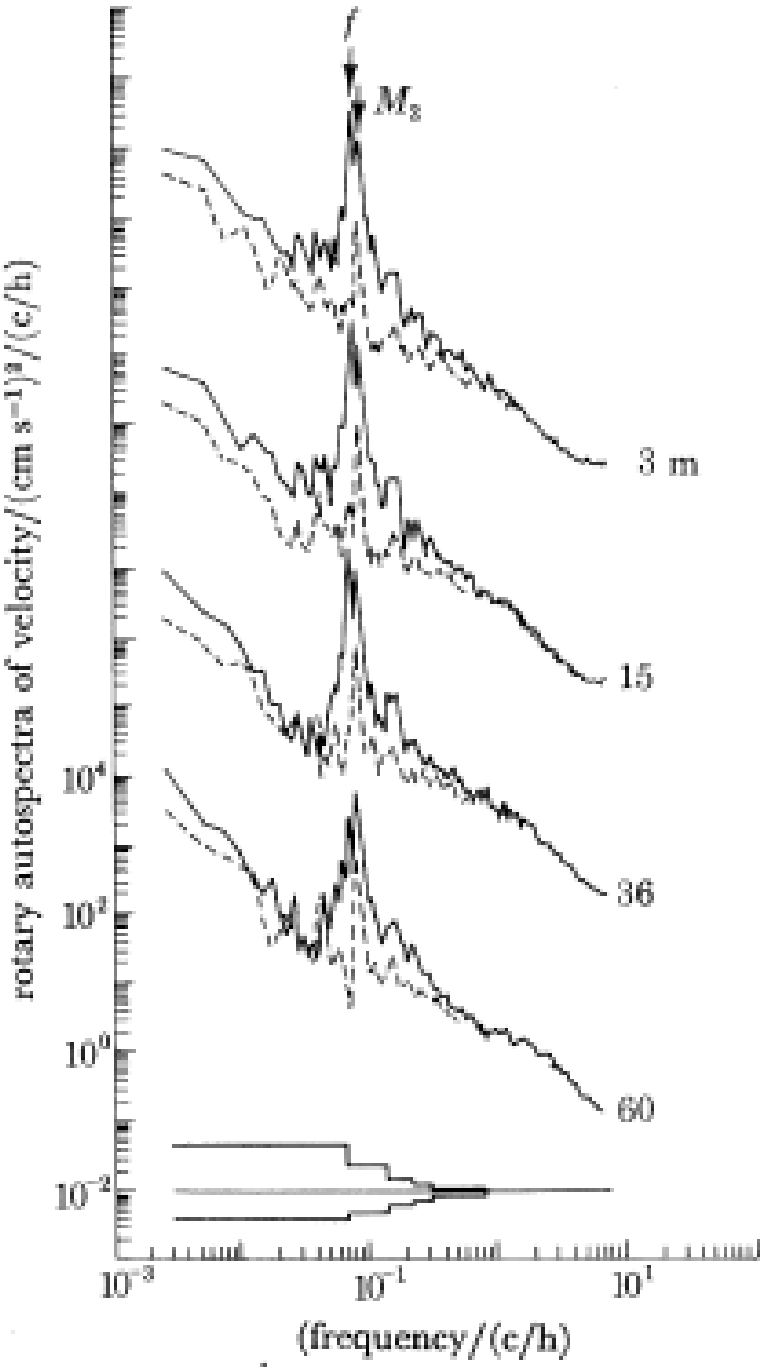

Moored time series of horizontal velocity: rotary autospectra of horizontal velocity at 3, 15, 36 and 60 m at a site in the northeastern Atlantic Ocean. Confidence limits (95 %) are shown below the spectra. The solid lines are the clockwise ($\omega < 0$) spectra, and the dashed lines are the counterclockwise ($\omega > 0$) spectra. The 3, 15, and 36 m spectra are plotted three decades above the spectrum from the next deepest record. The spectrum peaks are at tidal and Coriolis frequencies; higher frequencies are mostly internal waves and lower frequencies are mostly mesoscale eddies and response to low-frequency atmospheric wind forcing. (Weller and Halpern, 1983; repeated from earlier)

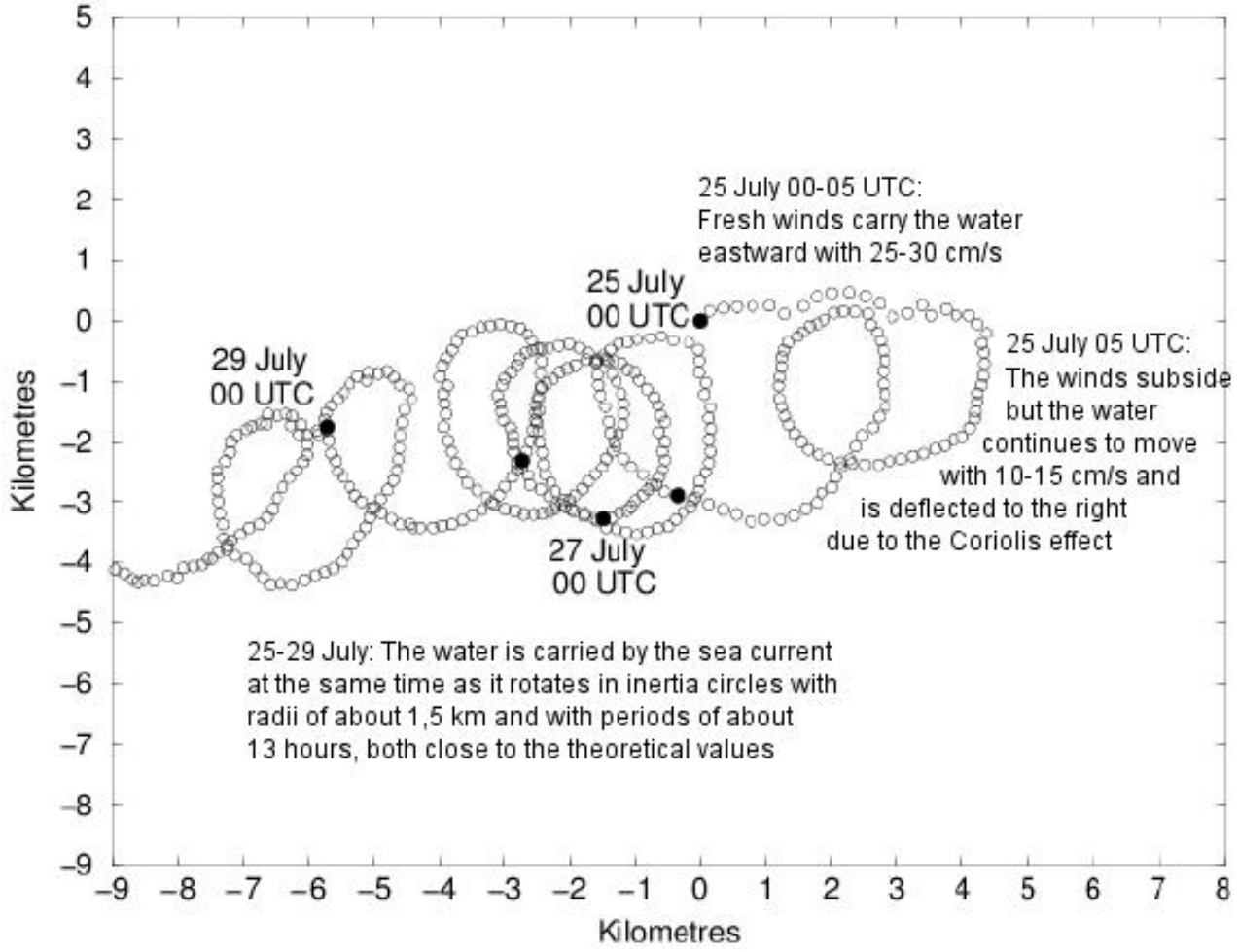

A drifting buoy set in motion by strong westerly winds in the Baltic Sea in July 1969. When the wind has decreased the uppermost water layers of the oceans tend to follow approximately inertial circles due to the Coriolis effect. In addition, low-frequency Ekman currents and mesoscale eddies cause a net drift so the trajectories are approximately cycloids. The inertial circles are not eddies but rather rotating currents on a large spatial scale: a set of buoys close to each other would be co-moving, rather than revolve around each other, because the horizontal correlation scale is large. (Web material by Cleon Teunissen)

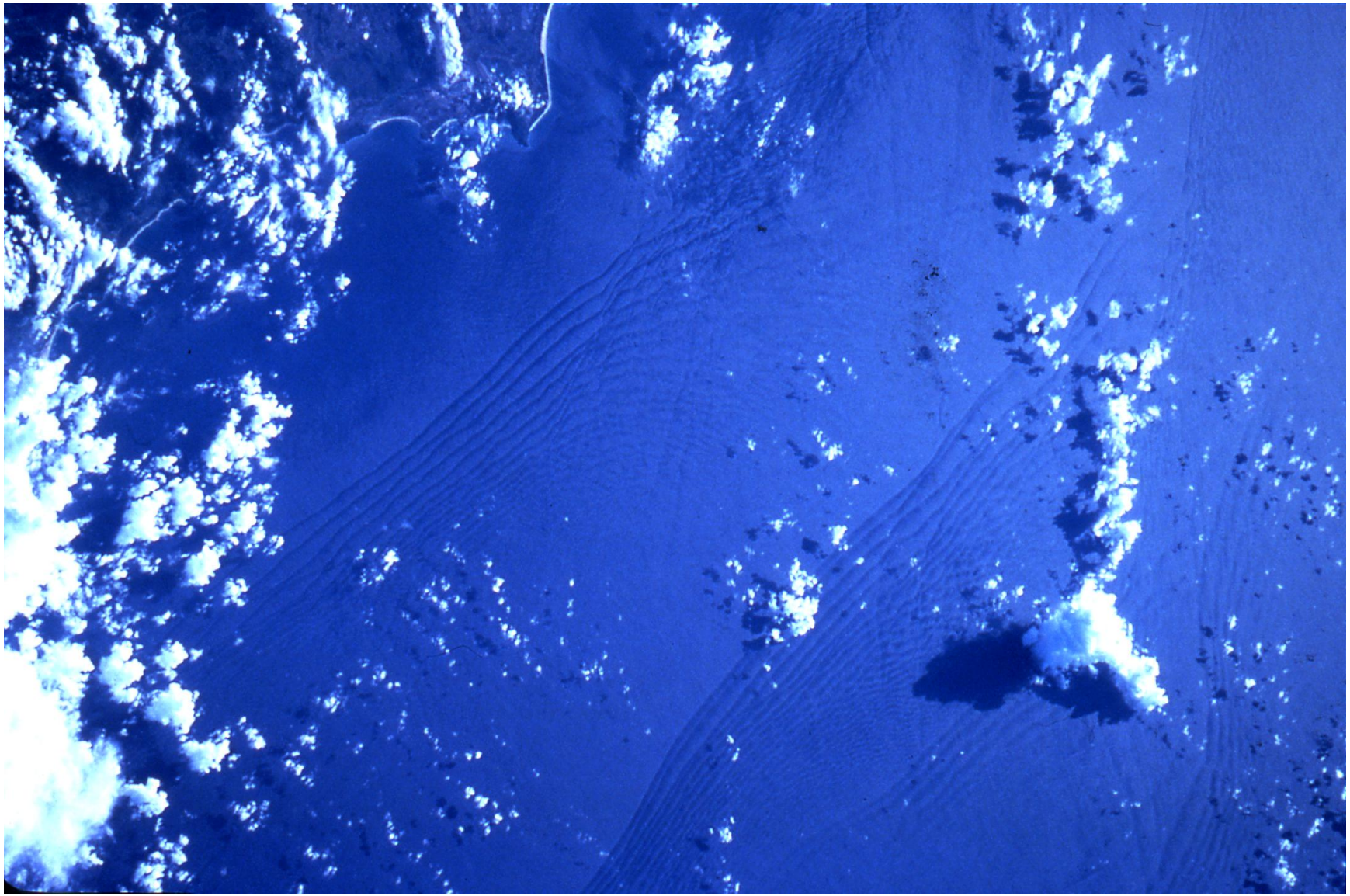

Photograph of the South China Sea showing internal tide crests and troughs (and clouds). Barotropic tide over undersea ridge generates a propagating inertia-gravity wave packet of large amplitude and approximately unchanging wave form over a distance of 1000 km ($i.e.$, a soliton). Pycnocline displacement amplitude is > 100 m.

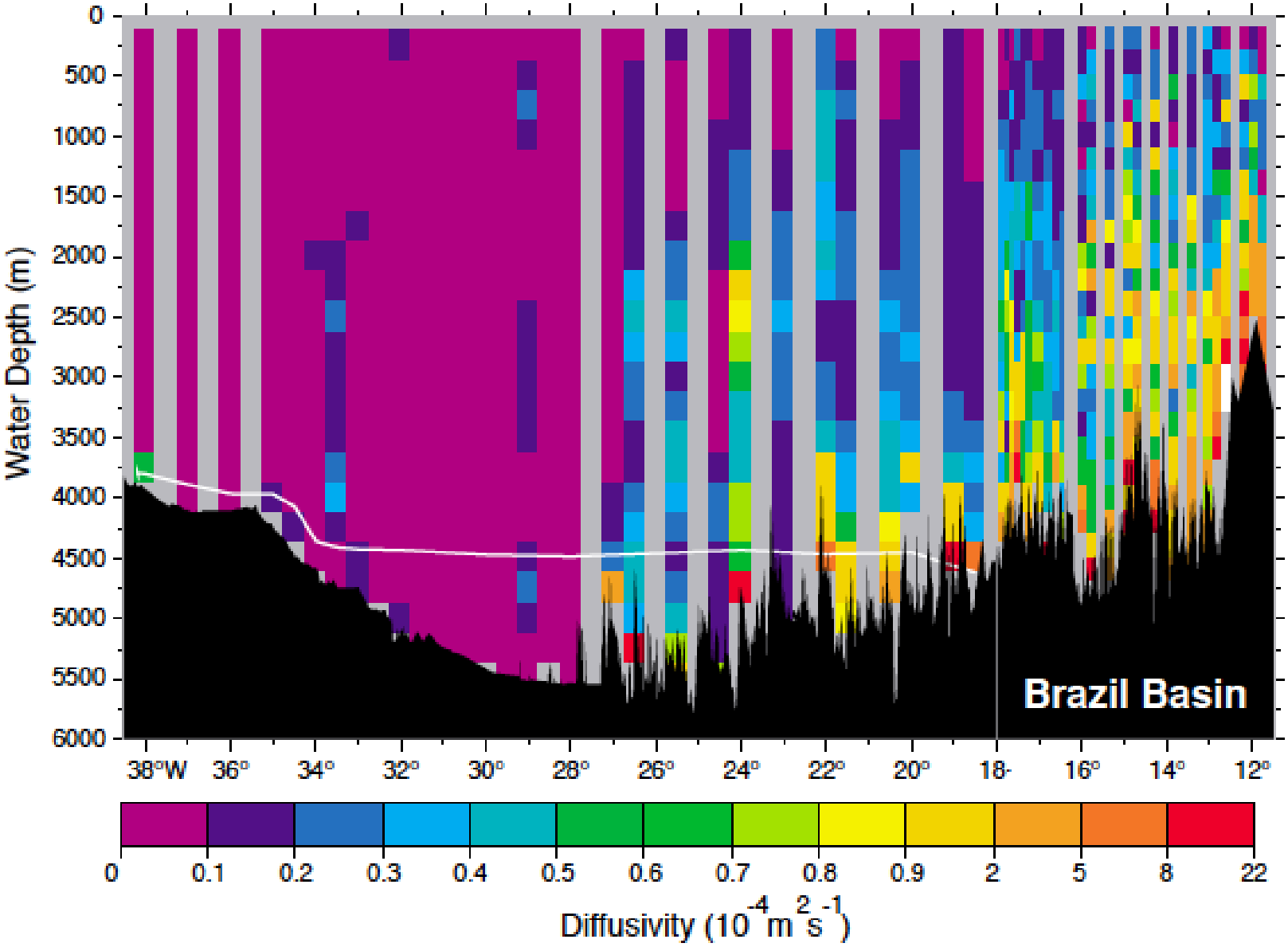

Vertical eddy diffusivity κ_v from micro-structure measurements in a zonal section across the Brazil Basin and Mid-Atlantic Ridge around 20 S. Enhanced values occur over rough topography through tidally generated internal waves that propagate upward, break, and mix. It is uncertain how much this penetrates into the pycnocline where typically $\kappa_v \sim 10^{-5}$ m^2 s^{-1}. (Polzin *et al.*, 1997)

Equatorial Kelvin Wave

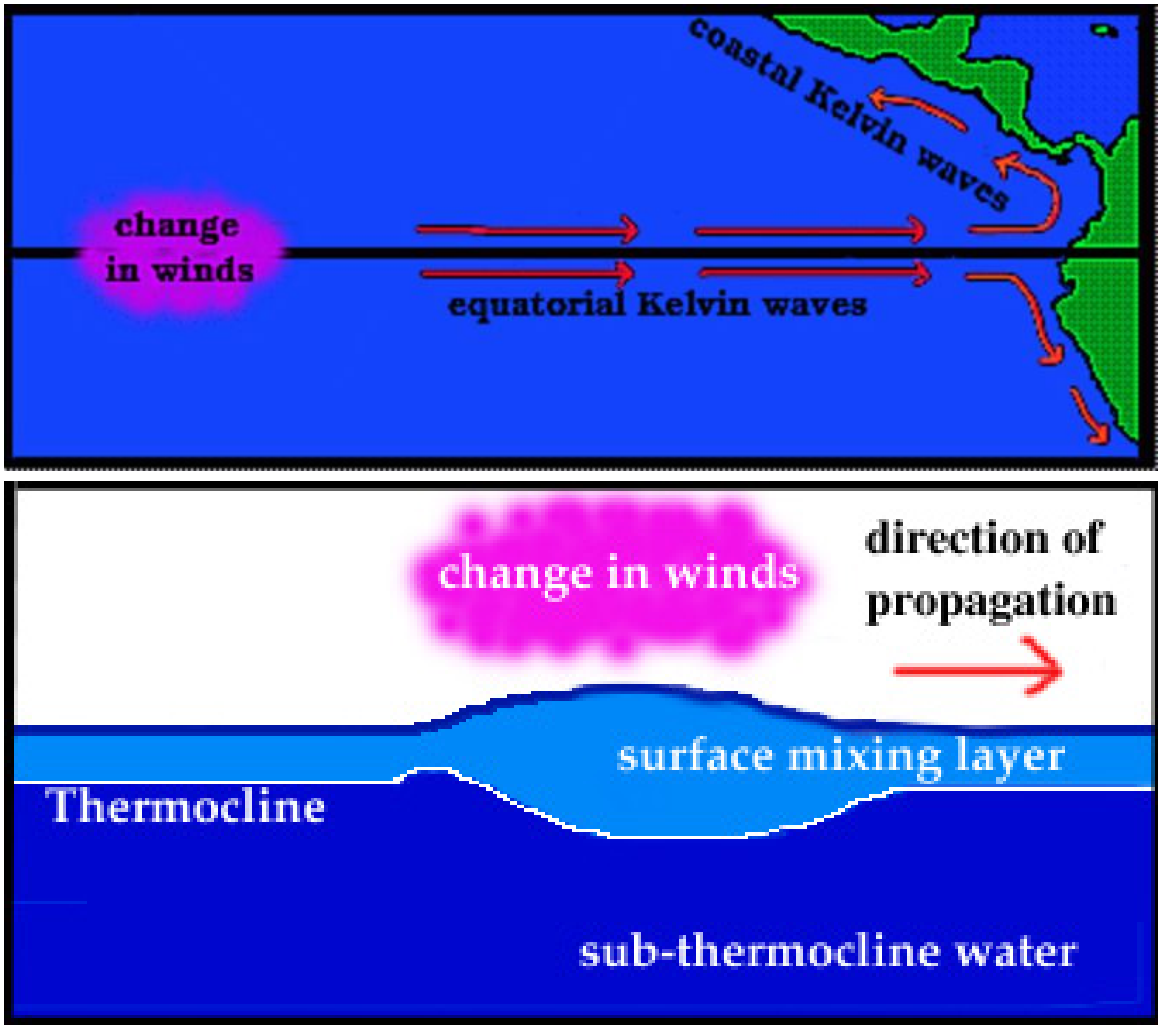

Equatorial Kelvin waves propagate to the east, using the equator zone as a wave guide. Coastal Kelvin waves propagate around the northern hemisphere oceans in a counterclockwise direction using the coastline as a wave guide. These waves are very fast moving, typically with speeds of 2.8 m/s near the Equator, or about 280 kilometers in a day. A Kelvin wave would take about 2 months to cross the Pacific from New Guinea to South America.

Rossby and Topographic Waves

Barotropic QG potential vorticity equation linearized around a resting depth $h(x, y)$:

$$\frac{DQ_{qg}}{Dt} = 0\,, \quad Q_{qg} = \zeta^{z\prime} + \overline{Q}_{qg}\,, \quad \overline{Q}_{qg} = \beta y - \frac{f_0}{h_0}\,h\,.$$

$$\Rightarrow\ \partial_t \zeta^{z\prime} + \beta v' - J[\psi', \frac{f_0}{h_0} h] = 0\,.$$

This has oscillatory "wave" solutions $\psi' \propto e^{i(\mathbf{k}\cdot\mathbf{x}-\sigma t)}$ with $\sigma \propto \nabla_h \overline{Q}_{qg} = \beta$ or $-(f_0/h_0)\,\nabla h$.

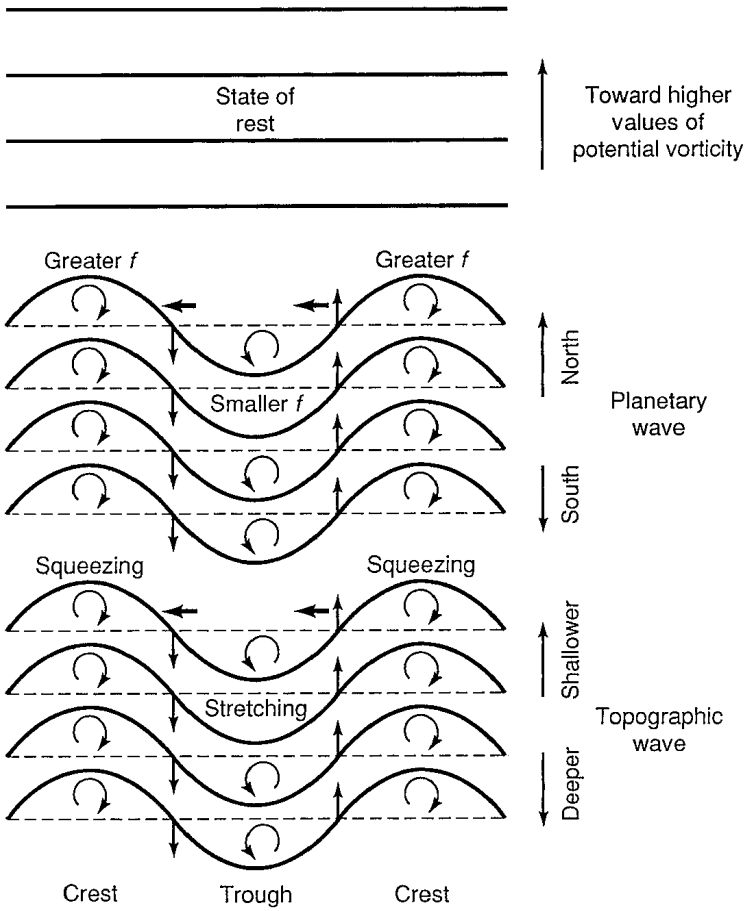

When a fluid parcel moves across $\overline{Q}_{qg}$ contours, it changes its vorticity ζ^z to conserve total Q_{qg}. This vorticity implies adjacent flow across $\overline{Q}_{qg}$ contours, causing them to change their vorticity, *etc.*. The net effect is a wave propagation of the vorticity centers along the $\overline{Q}_{qg}$ contours to the "west" or cyclonically within closed basis and anticyclonically around seamounts and islands, *i.e.*, with higher $\overline{Q}_{qg}$ to the right of the propagation path. (Figure from B. Cushman-Roisin)

Both steady current velocity and topographic Rossby waves propagation are along f/h contours.

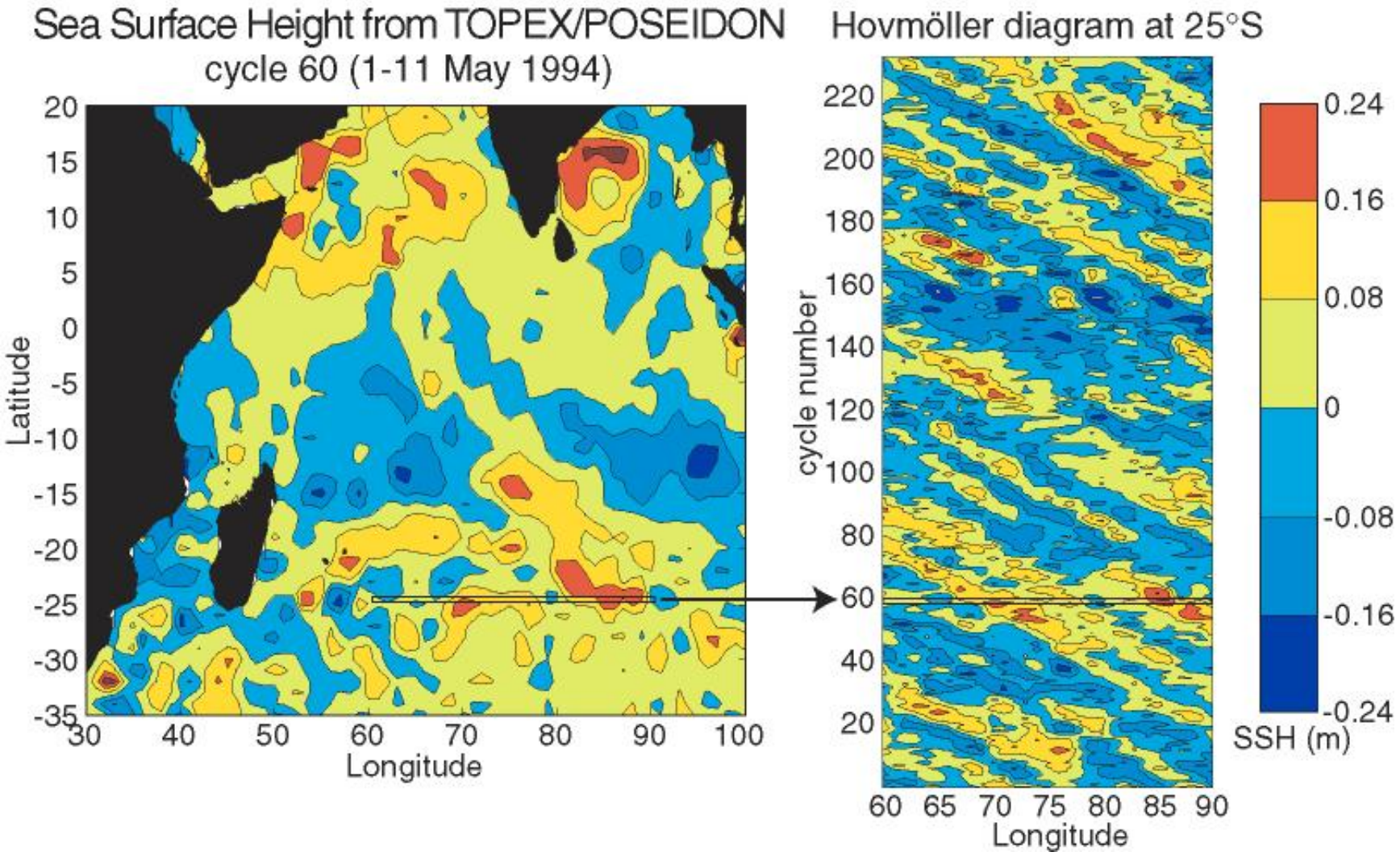

Sea surface height (SSH) from altimetry: (left) map of the Indian Ocean during an orbital-coverage cycle of ten days; (right) (x, t) diagram along 24 S over many cycles. Many of the features propagate westward with the speed of long baroclinic Rossby waves, $c^x = -\beta R_d^2$, where $R_d \approx NH/f$ is the baroclinic deformation radius ≈ 60 km at this latitude. Westward propagating occurs for both linear Rossby waves and nonlinear (rapidly recirculating, with $V/|c^x| \gg 1$) mesoscale eddies.

Barotropic and Baroclinic Instability

- QG instability of "mean" currents:

$$\frac{DQ_{qg}}{Dt} \approx 0\,, \qquad \psi \;=\; \overline{\psi} + \psi'\,, etc. \qquad \psi' \;\ll\; \overline{\psi} \qquad \Rightarrow$$

$$[\,\partial_t + \overline{\mathbf{u}}_g \cdot \nabla_h\,]\; Q'_{qg} + J[\psi', \overline{Q}_{qg}] \;\approx\; 0\,, \qquad \overline{Q}_{qg} = f(y) + \hat{\mathbf{z}} \cdot \nabla \times \overline{\mathbf{u}}_h + \partial_z(f\overline{b}/N^2)\,.$$

This can have exponentially growing eigenmodes, $\psi' \;\propto\; e^{\gamma t}$, $\gamma \sim V/L$ when either $\nabla_h \overline{u}$ or $\partial_z \overline{u}$ is large enough ($i.e.$, barotropic or baroclinic instability) and $\nabla_h \overline{Q}_{qg}$ changes sign somewhere (Rayleigh criterion).

- Unstable modes extract energy from the mean flow and limit its magnitude.
- Source of mesoscale eddies throughout the oceans, albeit non-uniformly.
- Especially strong in western boundary currents and Antarctic Circumpolar Current.
- Mesoscale eddies typically have the largest kinetic energy among all types of currents, and they are the dominant mixing agents for materials along isopycnal surfaces outside the BLs.
- Eddies have $L \approx R_d$ and vertical profiles mainly in the barotropic or first baroclinic mode ($i.e.$, nearly full depth).

Tropical Instability Waves (TIWs)

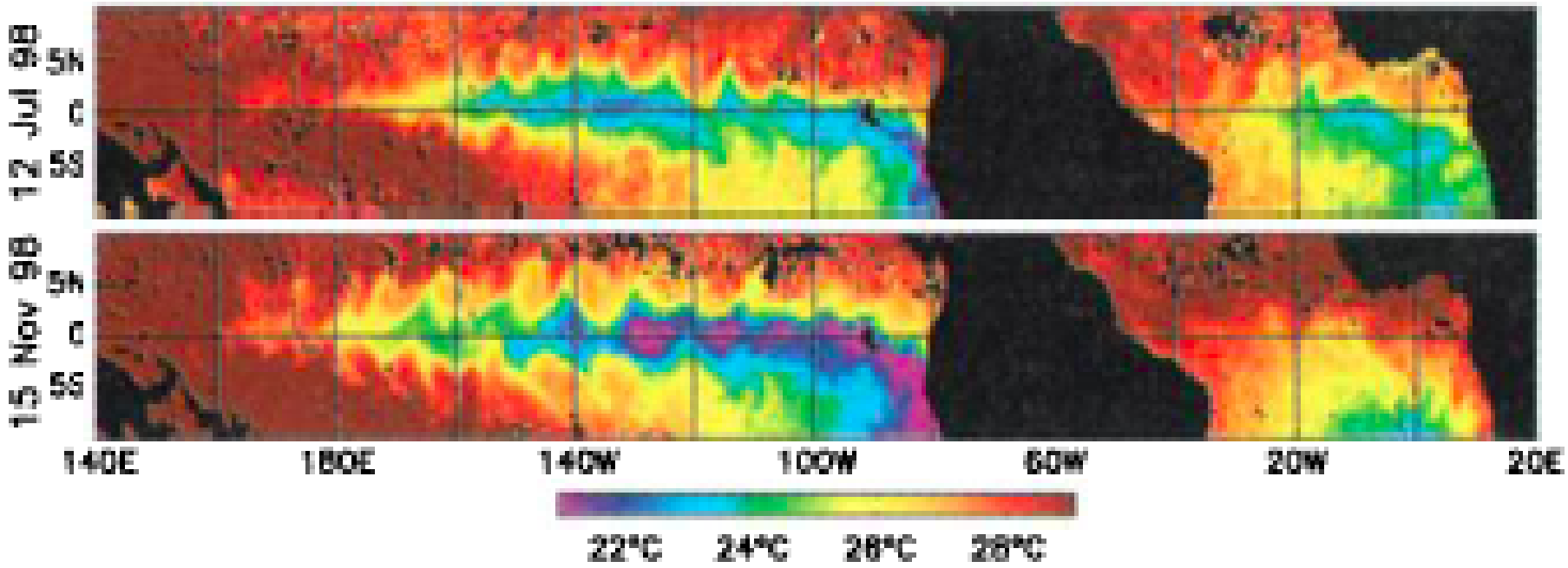

Snapshots of SST showing TIWs in the Pacific. They arise from barotropic instability of $\overline{u}(y,z)$, especially the shear on the equatorial side of the North Equatorial Counter Current. They are evident because of meridional currents displacing the northern edge of the equatorial cold tongue, *i.e.*, $T' \approx -(\int v'\,dt)\partial_y \overline{T}$. TIWs propagate westward with $c^x \approx -0.5$ m s^{-1}. The wave amplitude is large, and buoy trajectories show strong recirculation within the anticyclonic vortices between the SST cusps. (Chelton *et al.*, 2000)

Mesoscale Eddies and Geostrophic Turbulence

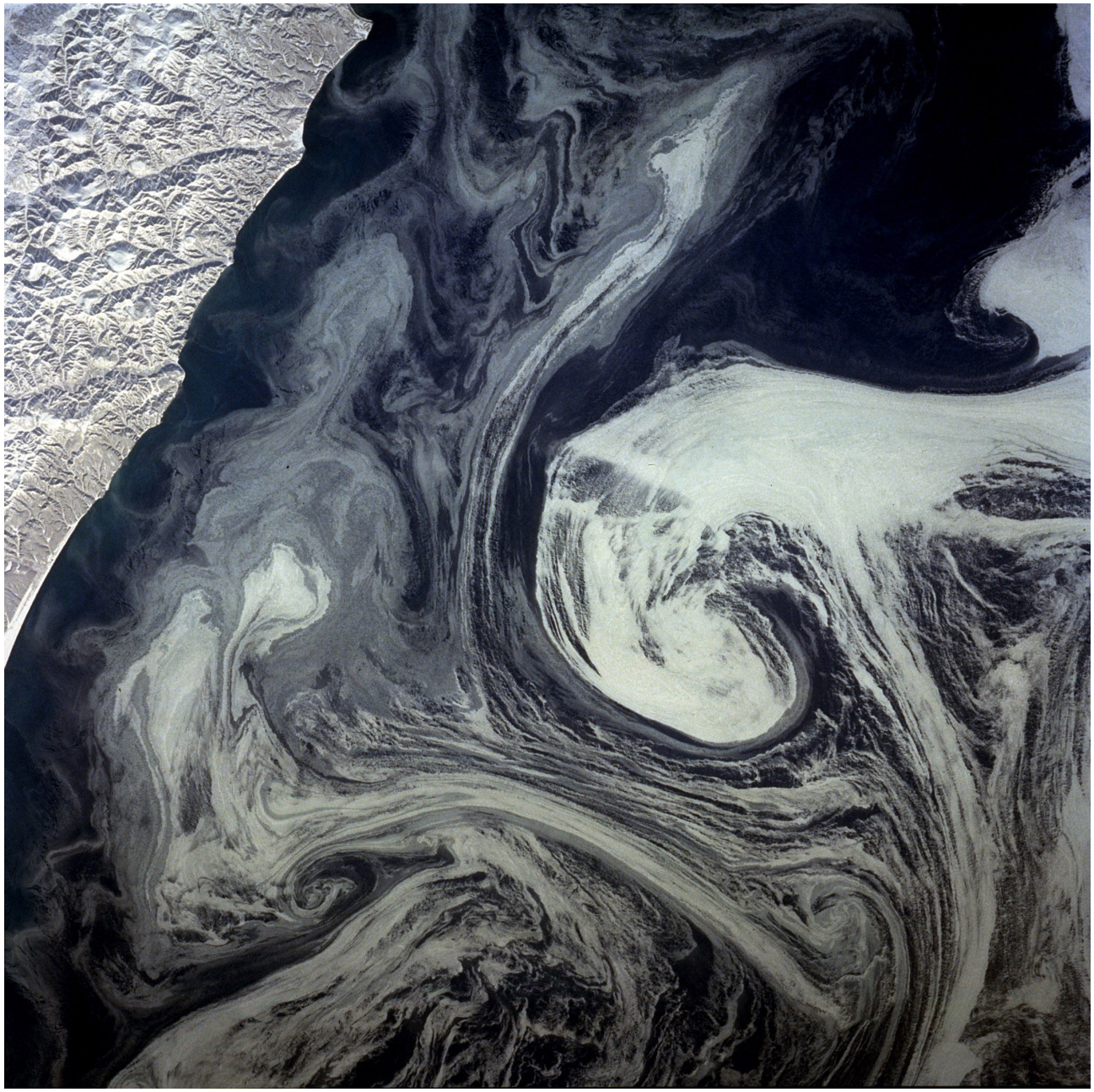

Eddy flow traced by fragmented sea-ice east of Greenland. The eddy $L \sim R_d \approx 25$ km. Many eddies are generated locally by baroclinic instability of the southward East Greenland current.

Eddy Kinetic Energy

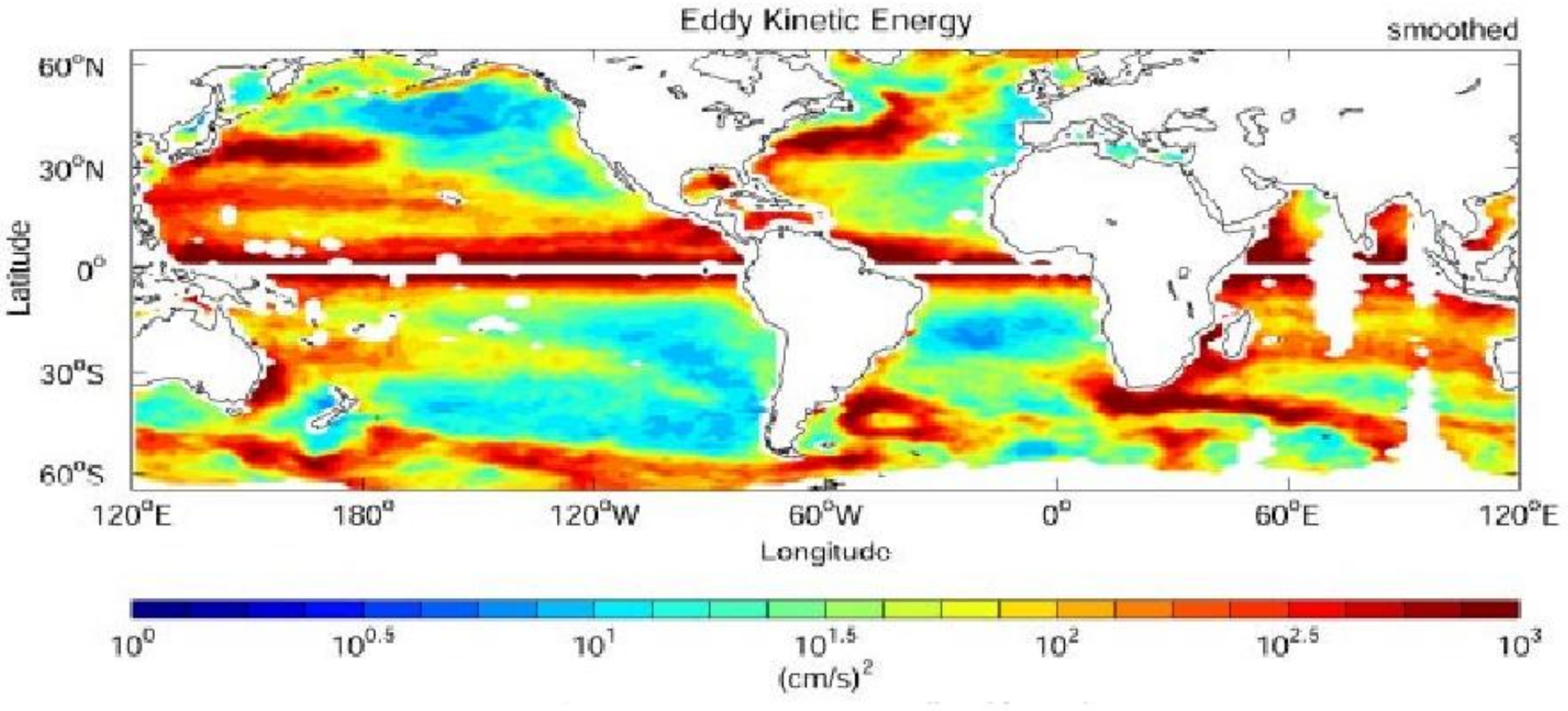

Mean eddy kinetic energy [$\mathrm{cm}^2\ \mathrm{s}^{-2}$] of geostrophic currents at the surface calculated from altimetric sea-level. Mostly this indicates mesoscale eddies. Notice the high energies where mean currents are strong: the tropics, western sides of gyres, and ACC. (Stammer and Scharfenberg, 2009; a repeated figure)

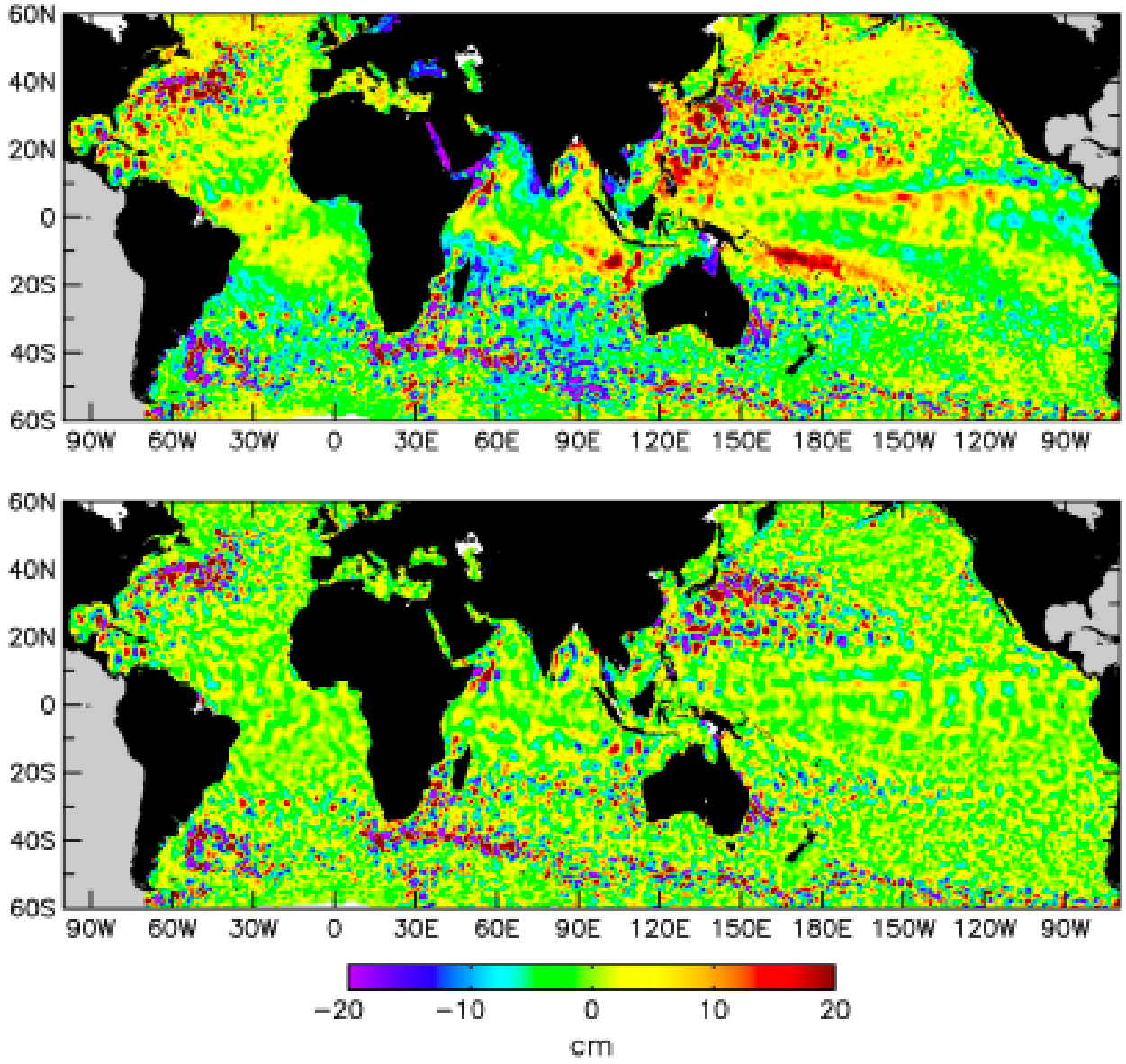

Example of a global altimetry SSH map (top) and a spatial high-pass filter at 20^o x 10^o to isolate the eddies from the larger-scale patterns (bottom). Automated eddy detection $\rightarrow$ 2495 "large" eddies with lifetime $\geq$ 1 month. Outside the tropics most eddies are nonlinear, with $V/\beta L^2 > 1$. Westward propagation is common, due to β, but not universal because of advection by mean currents and nearby eddies. (Chelton, 2011)

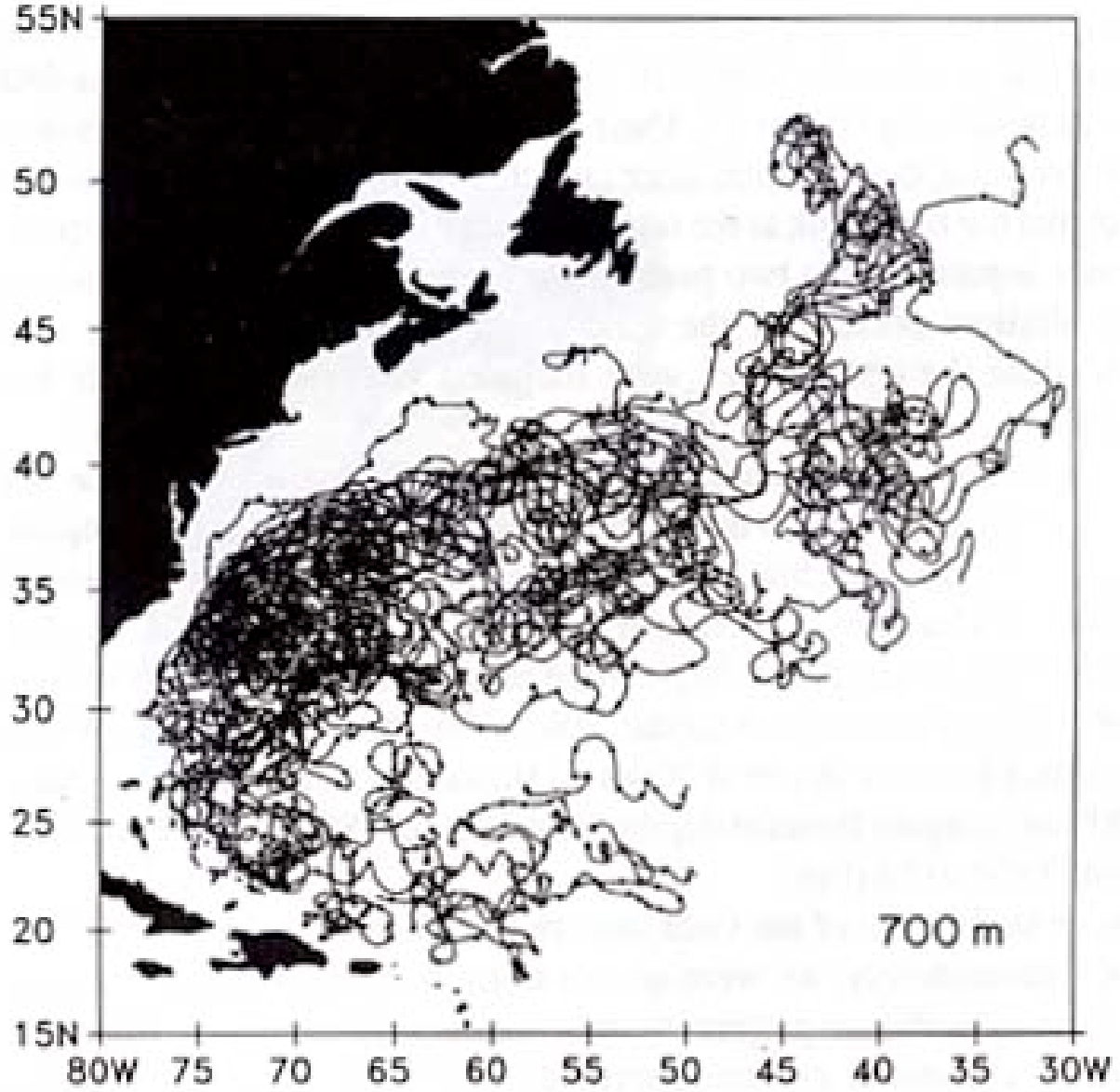

Trajectories for acoustically tracked neutrally buoyant floats at a nominal depth of 700 m in the Northwest Subtropical Gyre in the North Atlantic Ocean. Marks along trajectories occur at 30 day intervals. Note the general mixing and dispersion behaviors due to stirring by mesoscale eddies that transports materials mostly along isopycnal surfaces. (Owens, 1991).

Mesoscale-Induced Submesoscale Fronts

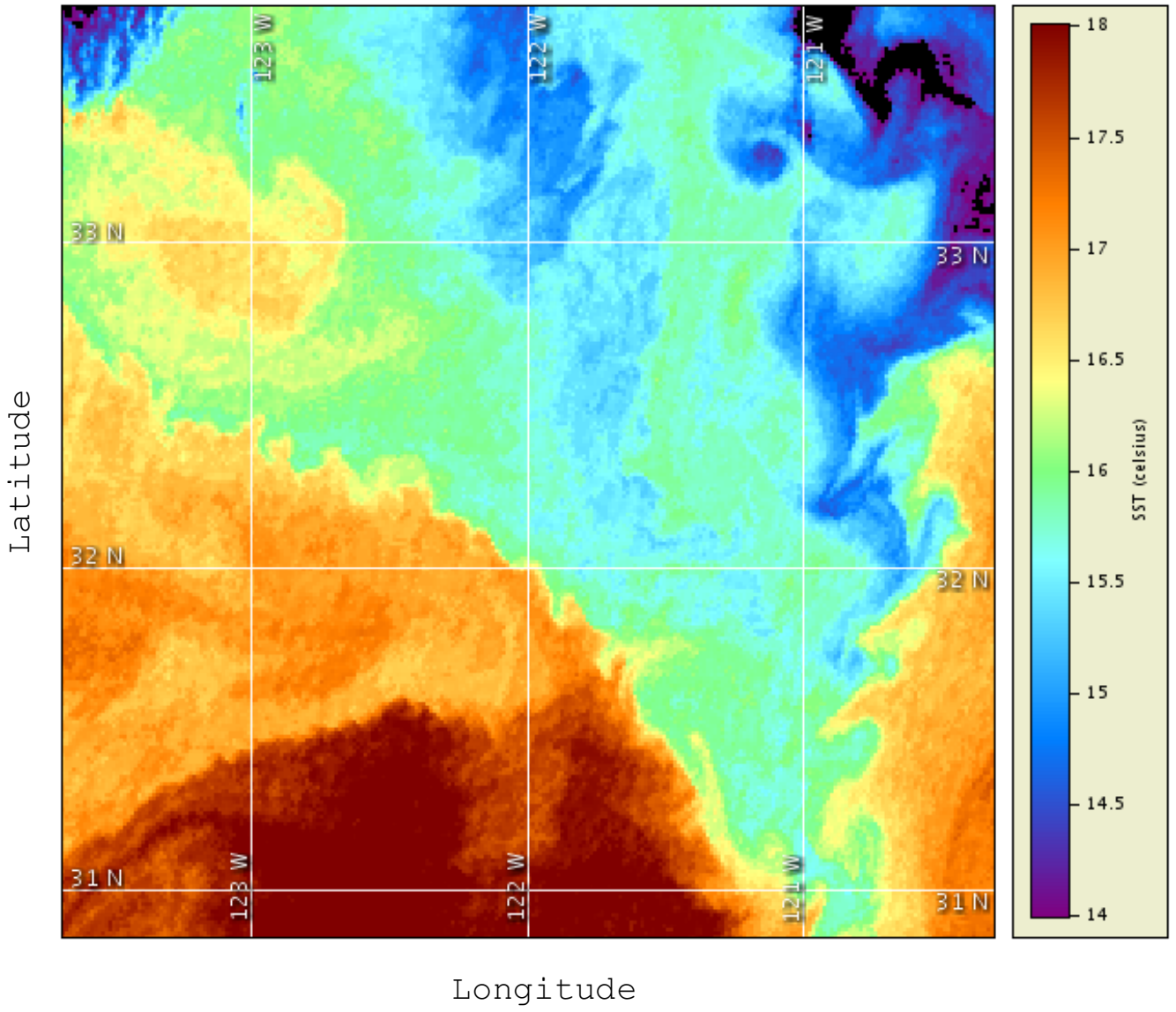

Satellite SST [^{o}C] image off California in $\sim (300\,km)^2$ domain (NOAA COASTWATCH).
Notice ~ 100 km mesoscale eddies and ~ 10 km submesoscale fronts with instabilities & vortices.
Frontogenesis; "mixed-layer baroclinic", ageostrophic, and centrifugal instabilities of upper ocean currents; and unstable topographic wakes are the primary sources of submesoscale energy.

Submesoscale Instabilities in the Gulf Stream

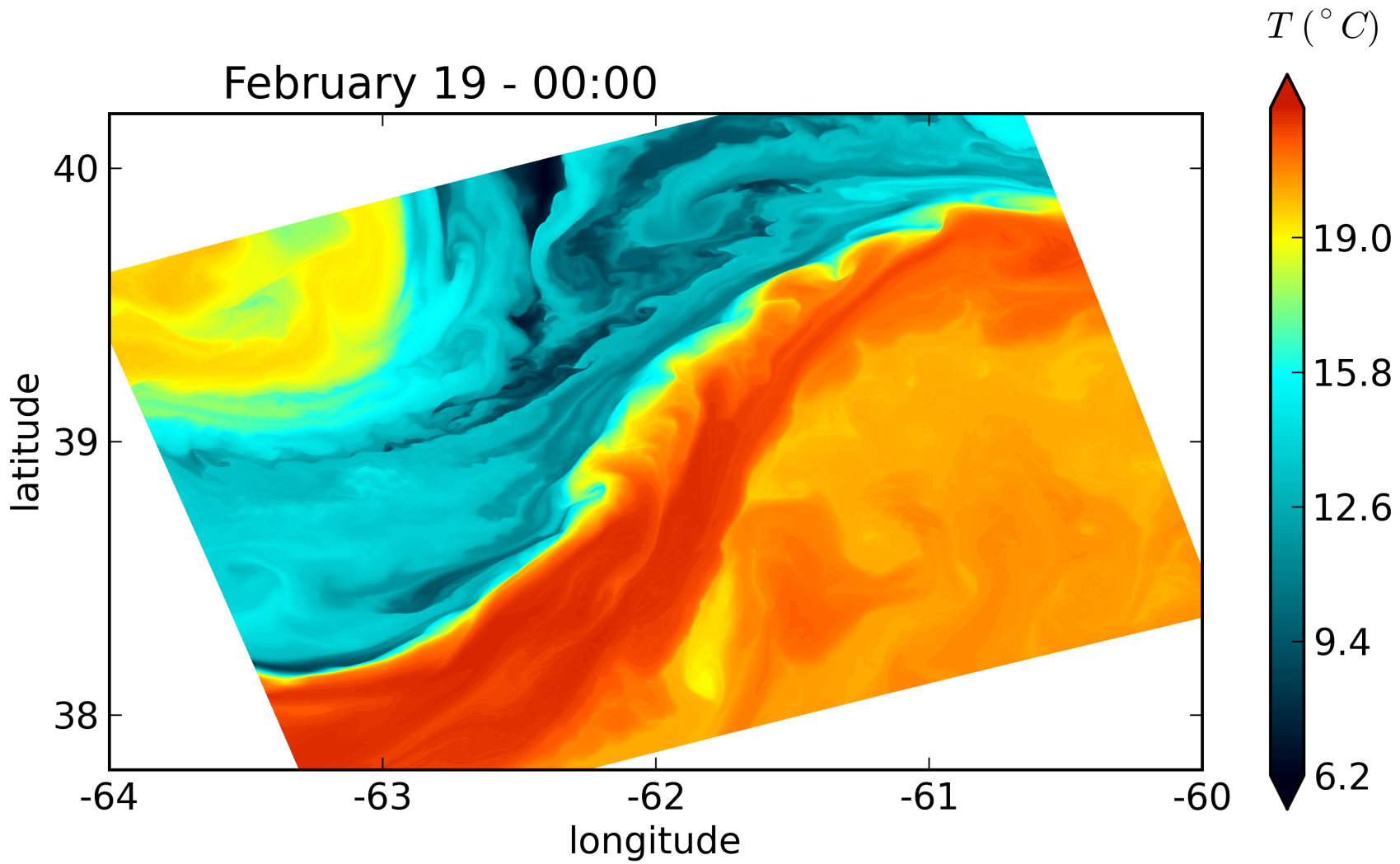

Simulated SST in an offshore sector of the Gulf Stream after separation from the western boundary. In addition to the meandering Core of the Stream and adjacent mesoscale eddy (called a Warm-Core Ring) that previously detached from the Stream, notice the submeoscale oscillations and cold-filament intrusions into the Core from the North Wall of the Stream. They act to decrease the warm Core going downstream by lateral mixing.

Wakes and Submesoscale Vortices

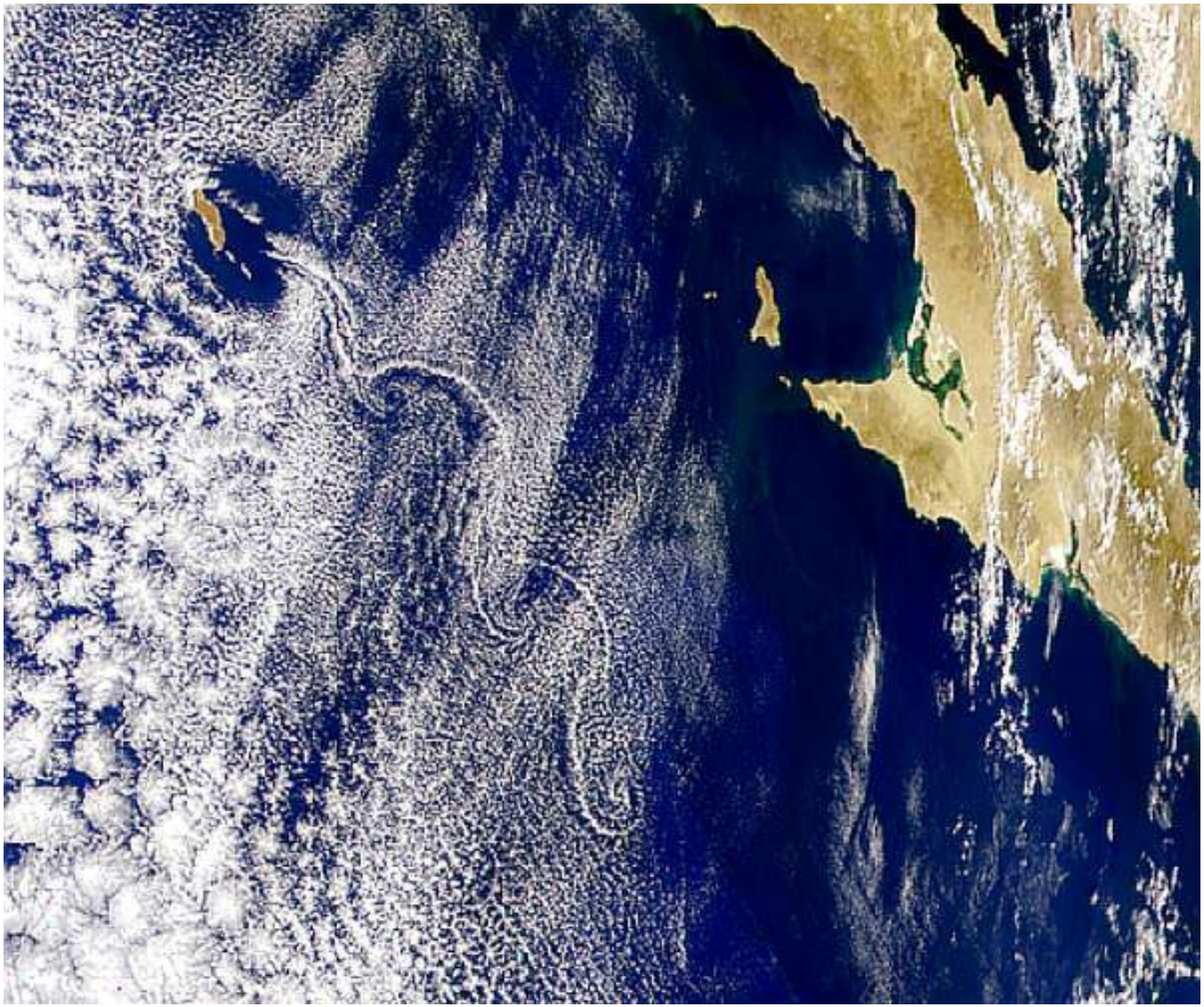

Flows past islands (as well as subsurface ridges) develop strong horizontal shear by drag against the sloping bottom. Past the island or ridge, it then separates as a wake, which is unstable and generates eddies. If the shear zone is narrow, then the eddies are submesoscale ($\sim$ 1-10 km). This example is an atmospheric wake behind Guadalupe Island west of Mexico with flow visualized by clouds; analogous wakes exist within the ocean.

Plankton Patchiness and Small scale circulations

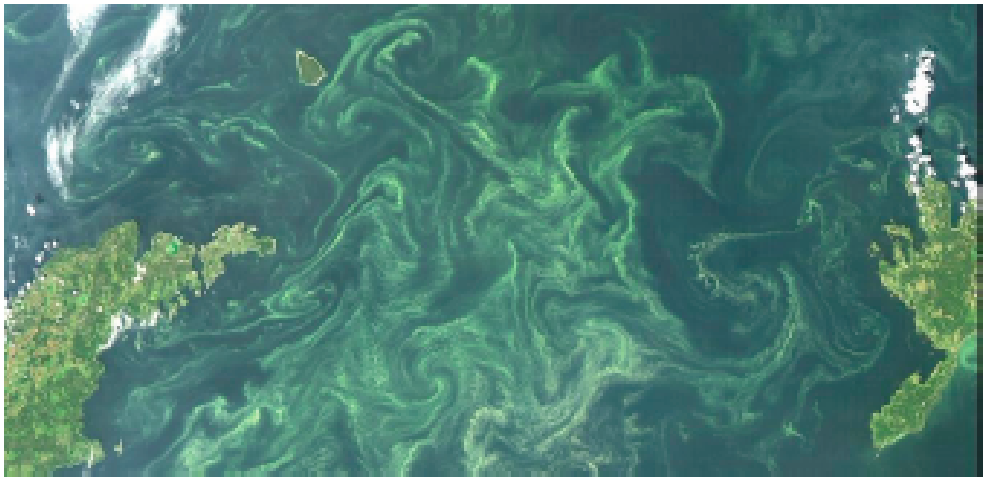

Plankton biomass is "patchy" - why?

Original ideas were diffusion oriented:

1) P growth is proportional to P
2) P is reduced by mixing/diffusion
3) Critical length scale for P to sustain

$$\frac{DP}{Dt} - \kappa \nabla^2 P = \mu P$$

$$L_{patch} \approx \sqrt{\frac{\kappa}{\mu}}$$

Problems with this view:

1) Scale-dependence of K
2) Much of the structure related to u,v,w → Eddies and fronts

In most of the mid-ocean away from coasts, mesoscale eddy "pumping" (transient uplift of isopycnals) may be the dominant source of nutrients in the euphotic zone, dominating boundary-layer turbulence, mean upwellling, and diapycnal mixing by internal waves and double diffusion. Within the surface layer submesoscale fronts and vortices may be the dominant source of w advection.

Submesoscale Surface Frontogenesis and Filamentogenesis

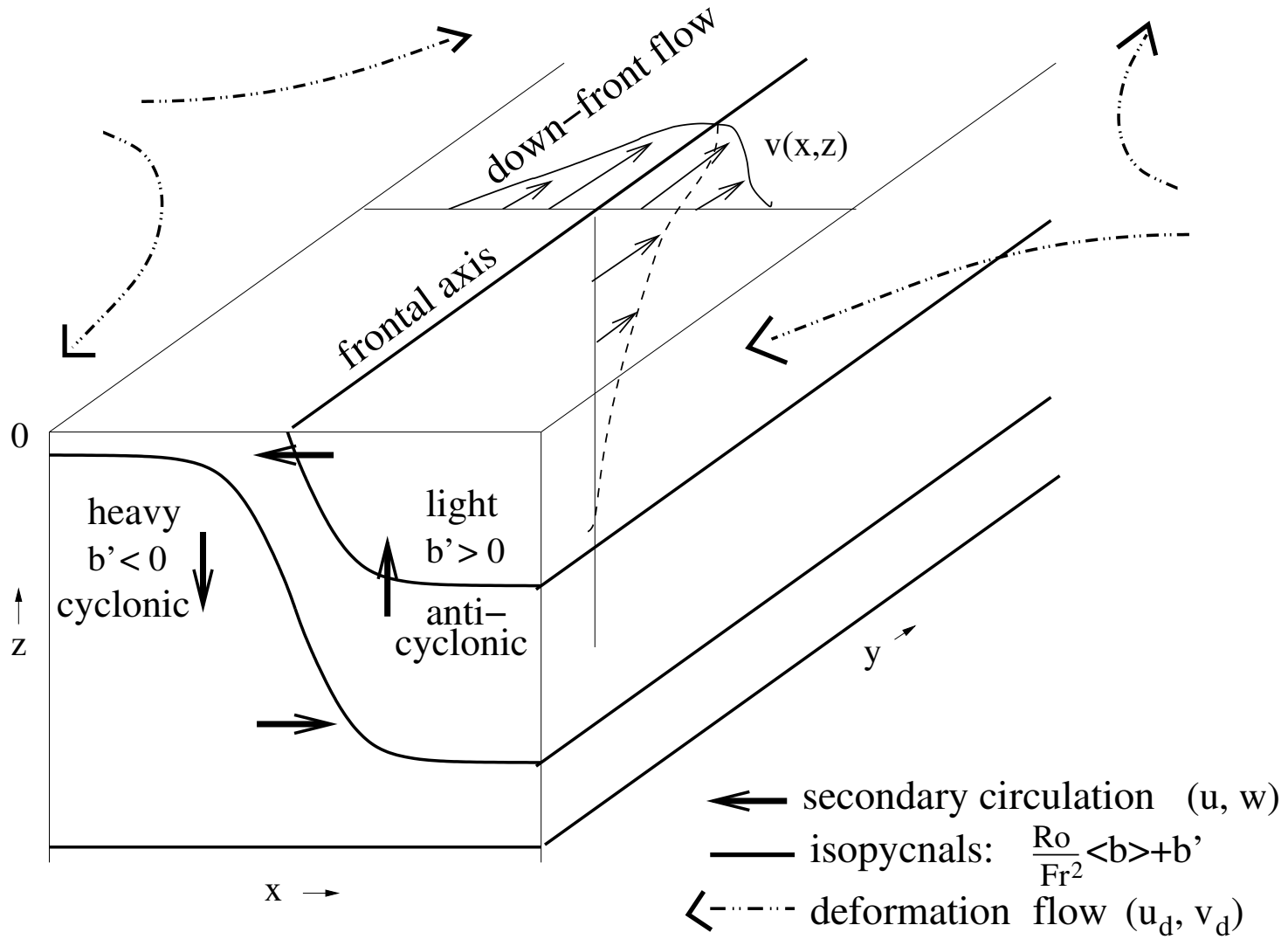

Flow configuration for 2D surface frontogenesis and secondary circulation induced by a mesoscale deformation flow. If $b(x, z = 0)$ has a extremum instead of a gradient, deformation flow causes filamentary intensification. These processes efficiently convert mesoscale $\rightarrow$ submesoscale. This phenomenon is similar in the atmosphere. Front = density gradient; Filament = density extremum.

Long-Lived Submesoscale Coherent Vortices (SCVs)

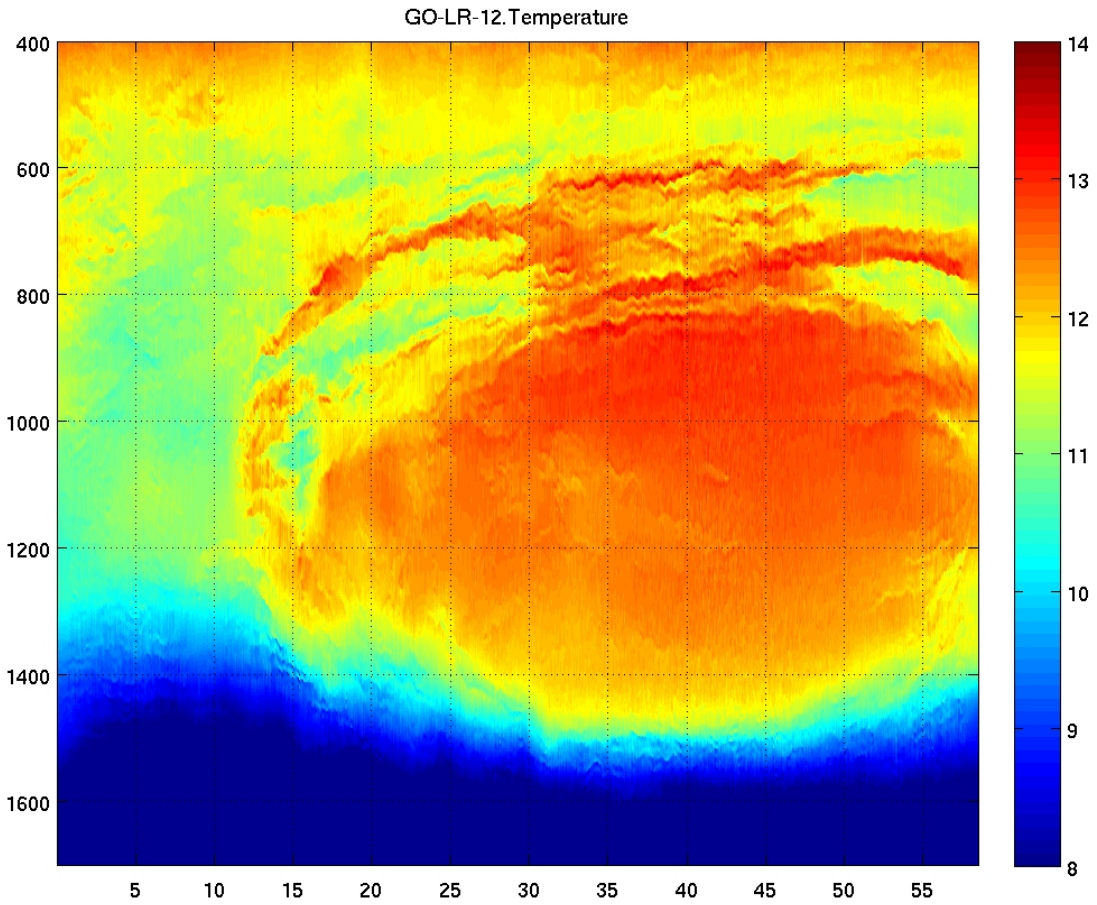

(r, z) cross-section of T [C] through a large-submesoscale Mediterranean Eddy (Meddy) measured by acoustic remote sensing in the Atlantic. The Meddy center is at 1100 m depth within the overflow mixing plume of dense, warm, salty water through Gibraltar Strait that then detaches from the boundary at its neutral buoyancy level. The density structure is a "lens" with isopycnals bulging upward above and downward below. The associated geostrophic velocity structure is an axisymmetric vortex with maximum speed at a radial distance of about 15 km. A Meddy SCV can survive for years as it moves around the North Atlantic. (Papenberg *et al.*, 2010)

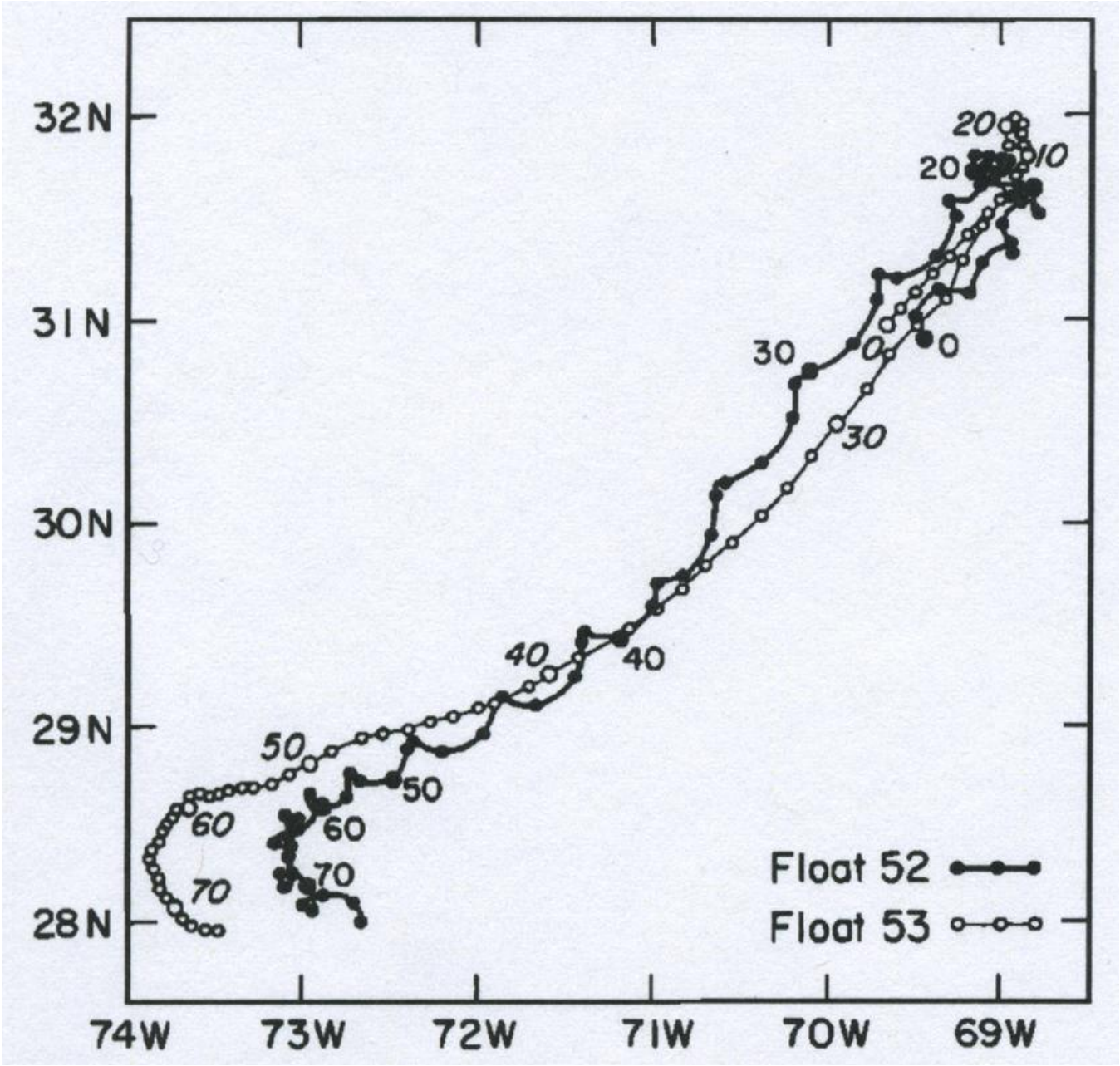

Trajectories of two neutrally-buoyant, acoustically-tracked floats at 700 m depth in the western subtropical North Atlantic. Time is labeled in days. Both floats move similarly due to the mesoscale current but one is released inside a SCV and recirculates many times. (Riser *et al.*, 1886)

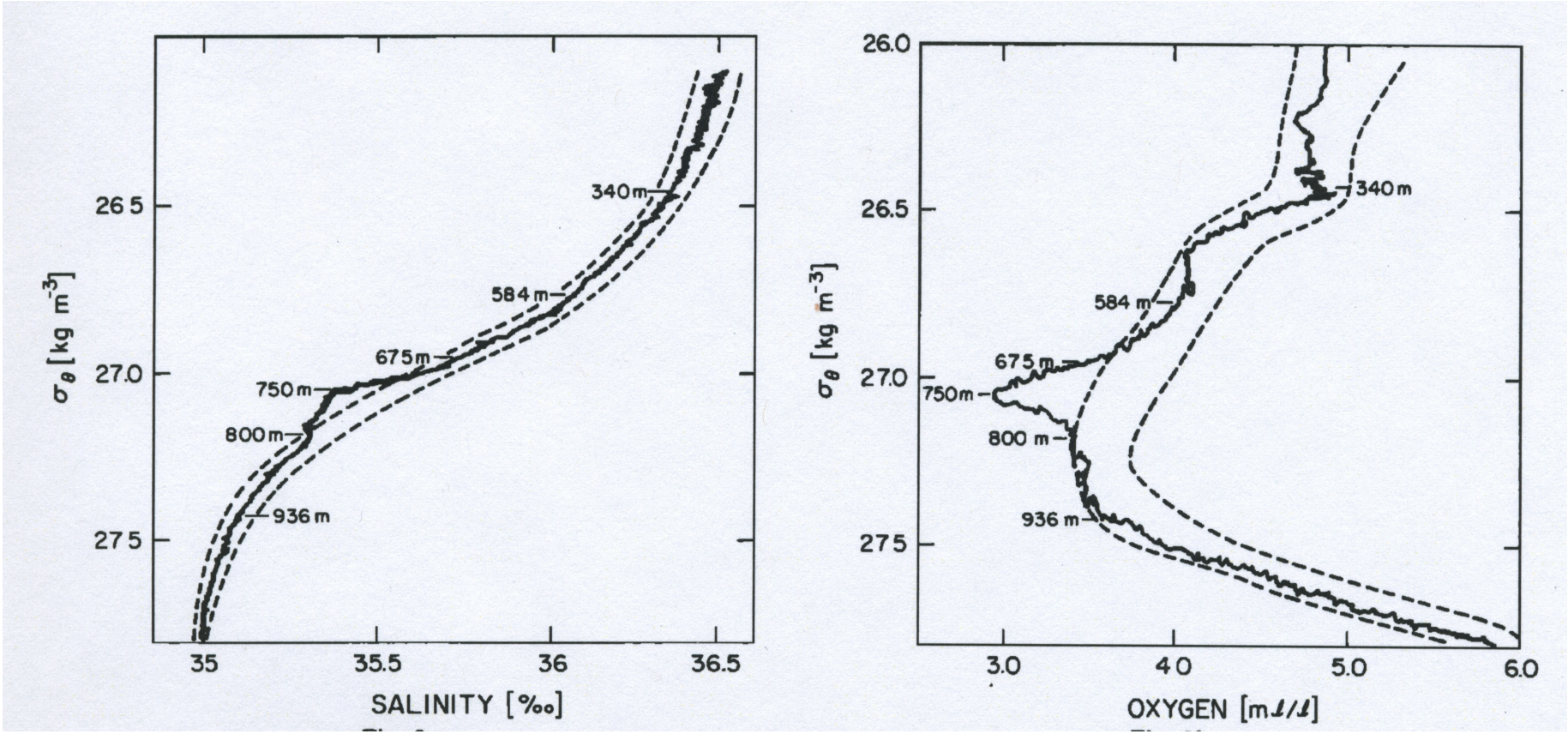

Hydrographic vertical profiles through the center of the preceding SCV. Dashed lines are mean $\pm\, 2\sigma$ local water-mass climatology, indicating the core water at 750 m is quite anomalous in S and O_2.

SCVs are "small", long-lived, abundant, sparse, mostly anti-cyclonic, and strong ($\partial_z \rho \to 0$, $\zeta^z \to -f$ in the center $i.e.$, $Q \to 0$ at marginal centrifugal instability).

SCV generation process is inferred as diapycnal mixing event in stratified water $\to$ geostrophic adjustment and axisymmetrization (sometimes as separating boundary currents; $e.g.$, Meddies, Cuddies [California Undercurrent], Swoddies [Slope Water]).

SCVs of many water-mass types have been found in many locations and depths, mostly by chance detection in sparse hydrographic profiles (as here).

Stratified Shear Instability and Microscale Turbulence

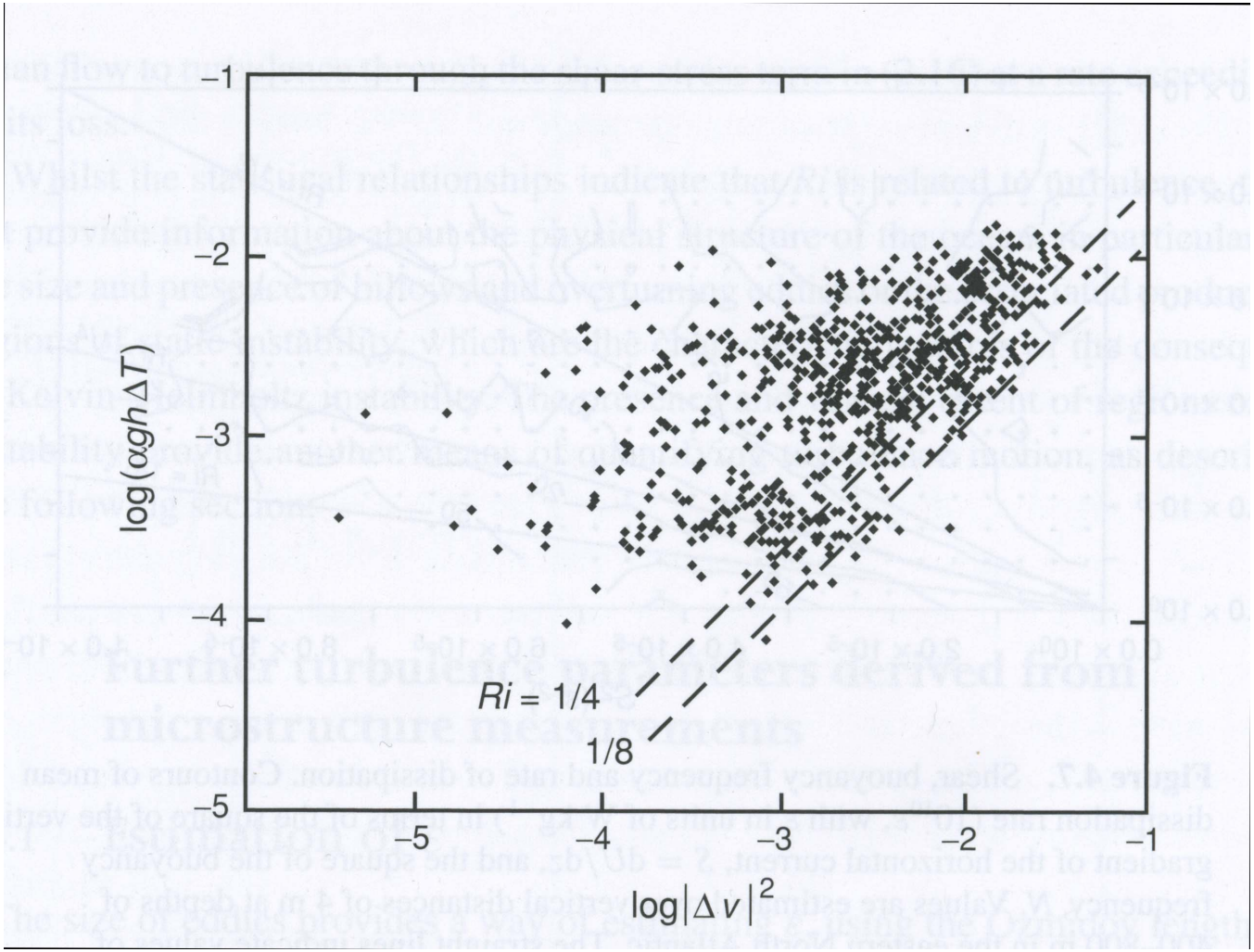

Vertical shear, temperature gradient, and $Ri = N^2/(\partial_z \mathbf{u})^2 \approx \tilde{\alpha} g \Delta z \Delta T/(\Delta v)^2$. A scatter plot of measured values over $\Delta z = 3$ m averaged over 110 s in the seasonal thermocline of the North Pacific. Notice how rare small Ri is; this reflects turbulent mixing efficiency by Kelvin-Helmholtz instability whenever $Ri \leq 0.25$, which weakens $\partial_z b$ and $\partial_z \mathbf{u}$ comparably, hence acts to increase Ri. (Thorpe, 2007). For $L \leq 100$ m and $H/L \ll 1$, stratified turbulence occurs without strong influence by f. This causes important diapycnal mixing outside the BLs.

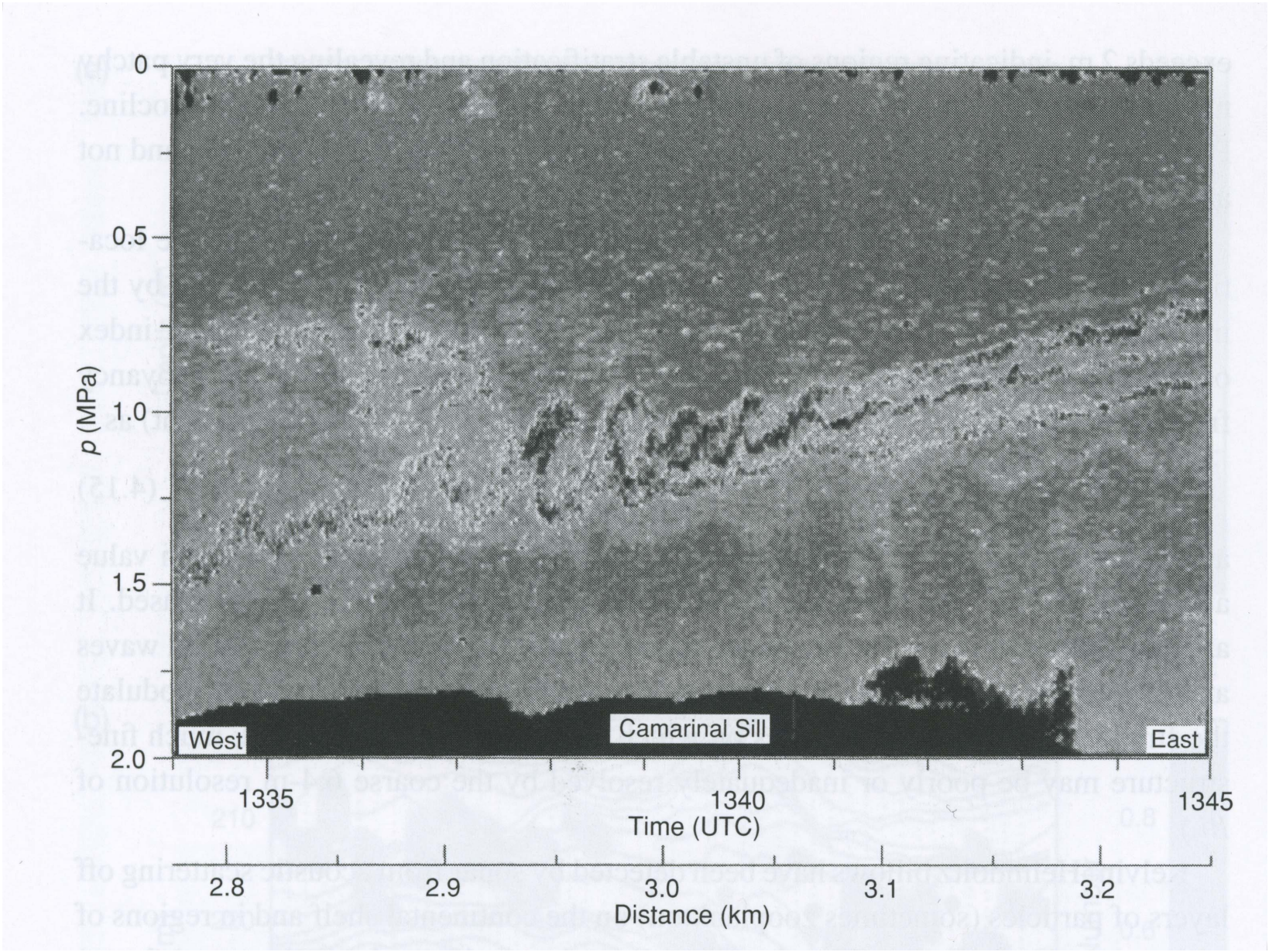

Kelvin-Helmholtz billows in the Strait of Gibraltar. The larger billows are about 25 m high around 125 m depth ($p = 1.25$ MPa). The background flow is eastward above and westward below with stable stratification, typical of the evaporation-driven exchange flow between the Atlantic and Mediterranean. (Thorpe, 2007) [also see movie at `http://en.wikipedia.org/wiki/File:KHI.gif`]

Double Diffusion: Salt Fingers and Diffusive Convection

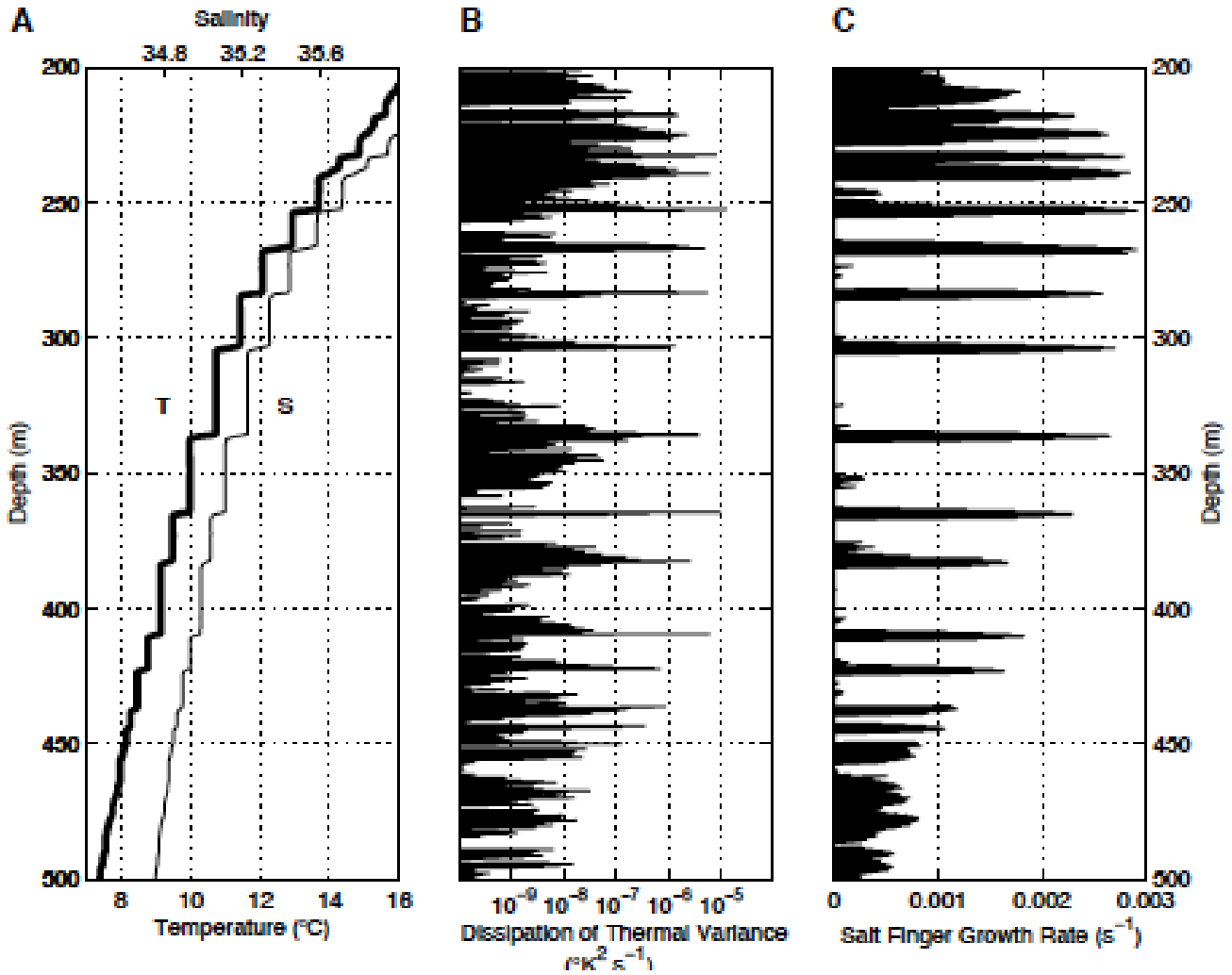

(A) Profiles of T and S; (B) T-variance dissipation rate $\epsilon_T = \kappa_T(\nabla T)^2$; and (C) salt finger growth rate in the Tropical Atlantic. The density ratio $R_\rho = \tilde{\alpha}\Delta T/\tilde{\beta}\Delta S \approx 1.5$ across interfaces $\Rightarrow$ $T - S$ staircase with warm, salty water above cold, fresh water and $N^2 > 0$ (*cf.*, cold, fresh above warm, salty with $R_\rho < 1 \Rightarrow$ diffusive convection). This is another important interior diapycnal mixing process. (Schmitt *et al.*, 2005)

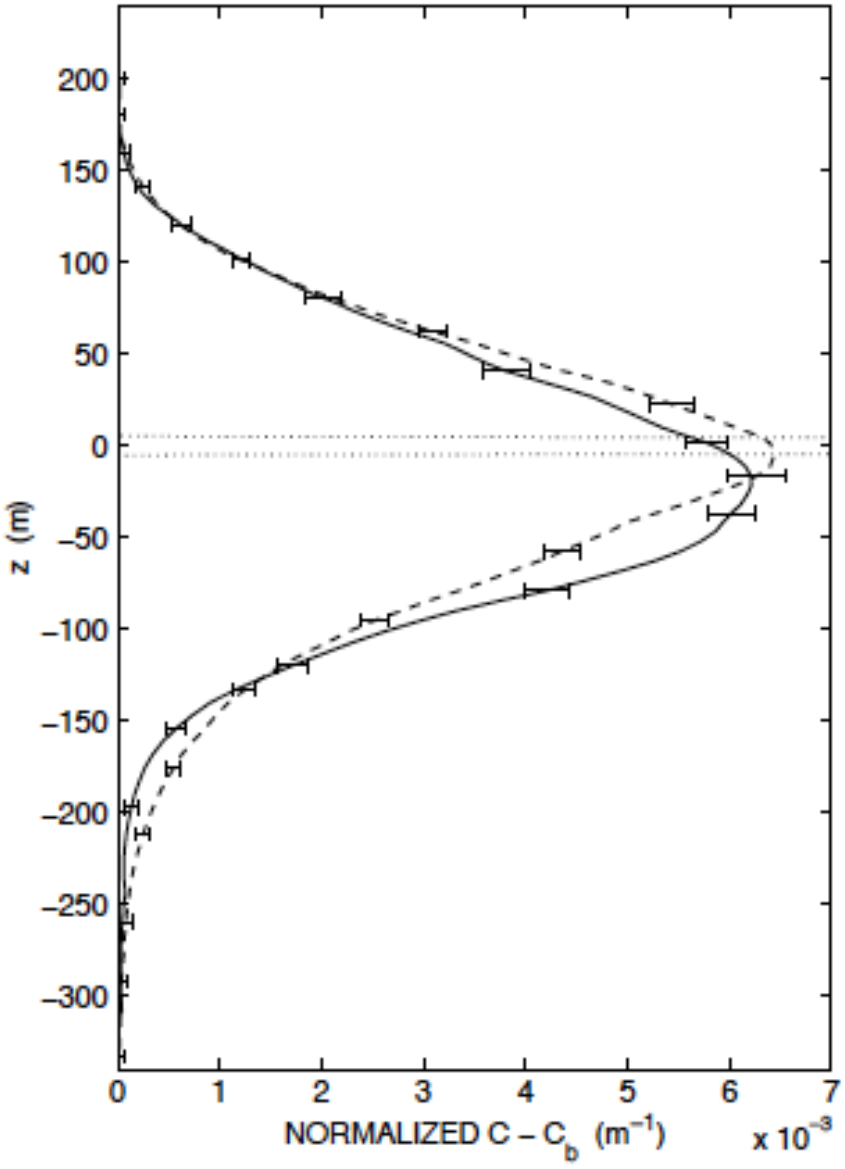

Fig. 3. Average vertical distribution of tracer about the injection density surface east of the Caribbean (solid line) and within the Caribbean Sea (dashed line) after 10 months. Tracer concentrations have been normalized such that the vertical integral is unity. The dotted lines delimit the initial tracer distribution. Averaging was done in density space, and the profiles were converted to physical space through the mean density profile for the stations east of Barbados.

Diapycnal mixing measured from the evolution of the vertical profile of an artifical tracer (SF_6) released on a single isopycnal surface in a salt-fingering regime. The spreading in z is assessed relative to the central isopycnal surface; diffusion $\rightarrow$ a profile $\sim \ t^{-1/2} \exp[-z'^2/4\kappa_v t]$ with a fitted spreading rate $\Rightarrow \kappa_v \approx 10^{-4}$ m^2 s^{-1}, nearly an order of magnitude larger than typical for the pycnocline. (Schmitt *et al.*, 2005)

Micro-Structure Turbulence

At the small-scale end of turbulent cascade, local kinetic energy and temperature variance balances assuming production = dissipation are

$$\begin{aligned} \overline{\mathbf{u}_h' w'} \cdot \frac{\partial \overline{\mathbf{u}}_h}{\partial z} &= \tilde{\alpha} g \, \overline{T' w'} - \epsilon \\ \overline{T' w'} \; N^2 &= -\frac{\tilde{\alpha} g}{2} \epsilon_T \, . \end{aligned}$$

Define eddy viscosity and diffusivity for vertical (diapycnal) mixing:

$$\nu_e = -\overline{\mathbf{u}_h' w'} \Big/ \frac{\partial \overline{\mathbf{u}}_h}{\partial z} \quad \text{and} \quad \kappa_e = -\tilde{\alpha} g \, \overline{w' T'} \Big/ N^2 \, .$$

$$\begin{aligned} \Rightarrow \quad \nu_e \left(\frac{\partial \overline{\mathbf{u}}_h}{\partial z} \right)^2 &= \frac{(\tilde{\alpha} g)^2 \epsilon_T}{2 N^2} + \epsilon \\ \kappa_e N^4 &= \frac{(\tilde{\alpha} g)^2}{2} \epsilon_T \, . \end{aligned}$$

This allows ν_e and κ_e to be inferred from micro-structure measurements of $\nabla \mathbf{u}'$, $\nabla T'$, $\partial_z \overline{\mathbf{u}}$, and $\partial_z \overline{T}$ to estimate ϵ and ϵ_T. $\tilde{\alpha}$ is the thermal expansion coefficient.

This technique is widely applied to estimate the small-scale oceanic mixing rate ($e.g.$, see Thorpe, 2007). κ_v is usually small in the pycnocline, $\nu_e \geq \kappa_e \approx 10^{-5}$ m^2 s^{-1}, with a few hoter spots (KH instability, salt-fingers, topgraphic boundary currents, $etc.$).

Concept: Oceanic GCMs are quite limited in the types of variability they can resolve, essentially limited to mean, seasonal, and interannual currents, mesoscale eddies (marginally), and tides (marginally), as well as the BGC signals on similar scales. Thus, the bulk of oceanic science lies outside of OGCMs.

This means that they are missing key processes that influence even the large-scale, low-frequency evolution, which therefore must be parameterized.

By present opinion the most important physics to parameterize are the following:

- mesoscale eddy isopycnal fluxes
- top and bottom boundary-layer vertical fluxes
- internal wave and double-diffusion diapycnal fluxes
- submesoscale surface layer restratification and BGC vertical fluxes
- kinetic energy dissipation in the interior
- diapycnal mixing over bottom slopes

This list is unlikely to change soon, although the parameterization schemes are evolving.

References

Chelton, D., F. Wentz, C. Gentemann, R. de Szoeke, and M. Schlax, 2000: Satellite Microwave SST observations of transequatorial Tropical Instability Waves. *Geophys. Res. Lett.* **27**, 11239-1242.

Chelton, D., 2011: Global observations of nonlinear mesoscale eddies. *Prog. Ocean.*, in press.

McWilliams, J.C., 1985: Submesoscale, coherent vortices in the ocean. *Rev. Geophys.* **23**, 165-182.

Owens, W.B., 1991: A statistical description of the mean circulation and eddy variability in the northwestern Atlantic using SOFAR floats. *Prog. in Oceanog.* **28**, 257-303.

Papenberg, C., D. Klaeschen, G. Krahmann, and R. W. Hobbs, 2010: Ocean temperature and salinity inverted from combined hydrographic and seismic data. *Geophys. Res. Lett.* **37**, L04601. doi:10.1029/2009GL042115.

Pedlosky, J., 2003: *Waves in the Ocean and Atmosophere*. Springer.

Polzin, K., K. Speer, J. Ledwell, and R. Schmitt, 1997: Spatial variability of turbulent mixing in the Abyssal Ocean. *Science* **276**, 93-96.

Riser, S., W. B. Owens, T. Rossby, and C. Ebbesmeyer, 1986: The structure, dynamics, and origin of a small scale lens of water in the western North Atlantic thermocline. *J. Phys. Ocean.* **16**, 572-590.

Schmitt, R., J. Ledwell, E. Montgomery, K. Polzin, J. Toole, 2005: Enhanced diapycnal mixing by salt fingers in the thermocline of the Tropical Atlantic. *Science* **308**, 685-688.

Thorpe, S., 2007: *An Introduction to Ocean Turbulence*. Cambridge Press.